Dalton Transactions

Synthesis, crystal structure, and cytotoxic activity of novel cyclic systems in (1,2,4)thiadiazolo[2,3-a]pyridine benzamide derivatives and their copper(II) complexes

Journal:	*Dalton Transactions*
Manuscript ID:	DT-ART-10-2013-052905.R2
Article Type:	Paper
Date Submitted by the Author:	21-Feb-2014

Complete List of Authors:
Adhami, forogh; Shahr ray Branch Islamic Azad Uni, Chemistry
safavi, Maliheh; Iranian Research Organization for Science and Technology, Biotechnology Department
Ehsani, Maryam; Shahr ray Branch Islamic Azad Uni, Chemistry
Ardestani, Susan; Institute of Biochemistry and Biophysics, Department of Biochemistry
Emmerling, Franziska; BMA Federal Institute for material research,
simyari, Farzaneh; Shahr ray Branch Islamic Azad Uni, Chemistry

Note: The following files were submitted by the author for peer review, but cannot be converted to PDF. You must view these files (e.g. movies) online.

Scheme 1 in revised manuscript.cdx
Scheme 2 in revised manuscript.cdx
Fig. 1 in revised manuscript. tif

Synthesis, crystal structure, and cytotoxic activity of novel cyclic systems in (1,2,4)thiadiazolo[2,3-a]pyridine benzamide derivatives and their copper(II) complexes

Forogh Adhami,*[a] **Maliheh Safavi**,[b] **Maryam Ehsani**,[a] **Sussan K. Ardestani**,[c] **Franziska Emmerling**,[d] **and Farzaneh Simyari** [a]

[a] *Department of Chemistry, Shahr-ray Branch, Islamic Azad University, PO Box 18155-144, Tehran, Iran, Fax: +982155229297; Tel: +9821552292; E-mail: fadhami@gmail.com*
[b] *Biotechnology Department, Iranian Research Organization for Science and Technology, Tehran, Iran*
[c] *Institute of Biochemistry and Biophysics, Department of Biochemistry, University of Tehran, PO Box 13145-1384, Tehran, Iran*
[d] *BAM Federal Institute for Materials Research and Testing, Berlin, Germany*
[e] *Pharmaceutical Sciences Research Centre, Tehran University of Medical Sciences, Tehran 14174, Iran*

Abstract

Three *N*-(pyridine-2-ylcarbamothioyl)benzamide derivatives were synthesized by the reaction of potassium thiocyanate, benzoyl chloride, and 2-amino pyridine derivatives in one pot. The obtained derivatives were oxidized using copper(II) chloride. During the oxidation, two hydrogen atoms were removed, cyclization of the derivatives occurred, and finally, three new *N*-(2H-[1,2,4]-thiadiazolo[2,3-a]pyridine-2-ylidne)benzamide derivatives were produced. Coordination of these three new derivative ligands to copper(II) ion resulted in the formation of three new complexes: dichlorobis(*N*-(2H-[1,2,4]thiadiazolo[2,3-a]pyridine-2-ylidene)benzamide)copper(II), dichlorobis(*N*-(7-methyl-2H-[1,2,4]thiadiazolo[2,3-a]pyridine-2ylidene)benzamide)copper(II), and dichlorobis(*N*-(5-methyl[1,2,4]thiadiazolo[2,3-a]pyridine-2-ylidene)benzamide)copper(II). All the synthesized products were characterized by IR, ^{1}HNMR, and ^{13}CNMR spectroscopies. Crystal structures of the obtained *N*-(pyridine-2-ylcarbamothioyl)benzamide derivatives, *N*-(2H-[1,2,4]-thiadiazolo[2,3-a]pyridine-2-ylidne)benzamide derivatives, and complexes were determined using X-ray single-crystal diffraction; the position of atoms, bond lengths, bond angles, and dihedral angles were also determined. In all complexes, the coordination of two large monodentate ligands and two chloride anions to copper(II) ion resulted in the formation of a stable planar geometry around the central ion. Three *N*-(pyridine-2-ylcarbamothioyl)benzamide derivatives, three *N*-(2H-[1,2,4]-

thiadiazolo[2,3-a]pyridine-2-ylidne)benzamide derivatives, and three complexes were evaluated for their cytotoxicity against five human cancer cell lines (breast cancer cell line MDA-MB-231, neuroblastoma cell line SK-N-MC, prostate adenocarcinoma cell line LNCap, nasopharyngeal epidermoid carcinoma cell line KB, and liver cancer cell line HEPG-2) using an *in vitro* analysis. The *N*-(pyridine-2-ylcarbamothioyl)benzamide derivatives showed no cytotoxic activity, whereas the *N*-(2H-[12,4]-thiadiazolo[2,3-a]pyridine-2-ylidne)benzamide derivatives and their complexes showed significant cytotoxicity, especially against MDA-MB-231 and LNCap cell lines. The complexes demonstrated smaller IC_{50} values than *N*-(2H-[1,2,4]-thiadiazolo[2,3-a]pyridine-2-ylidne)benzamide derivatives.

1. Introduction

Cancer, as a major health disorder, is responsible for more than 20% of the world's mortality. Therefore, development of processes for the prevention and treatment of cancer is becoming more important than ever. Medicinal chemistry, with a long history of improvement of drug families to treat cancer, has made it to its goal of developing efficient anticancer agents for the treatment of various cancers.

Benzamide derivatives and their substitutes, with diverse and interesting structures, have been shown to be pharmacologically active in the treatment of different diseases such as cancer [1–4]. Metoclopramide (MCA) as a benzamide derivative has been reported to enhance the effects of cisplatin and ionizing radiation on xenografted human squamous cell carcinomas of the head and neck region [5, 6]. Further, several benzamide compounds synthesized from anacardic acid, with cytotoxicity effect on a HeLa cell line of wild type, have been reported to have anticancer and anti-inflammatory properties; examples include 2-isopropoxy-6-pentadecyl-N-pyridin-4-ylbenzamide, 2-ethoxy-N-(3-nitrophenyl)-6-pentadecylbenzamide, and 2-ethoxy-6-pentadecyl-N-pyridin-4-ylbenzamide, with respective IC_{50} values of 11.02, 13.55, and 15.29 μM [7, 8]. Cyano(acrylamido)benzamide has been reported to exhibit antitumor activity against breast carcinoma cell line [9]. In addition, cyano(phenyl)(hexahydroquinoline-2-yl)benzamide has shown potent cytotoxicity against hepatic cancer cells [10]. Halogen derivatives of oxoindolin-3-ylideneaminobenzamide have been reported to exhibit moderate cytotoxic activity against human breast adenocarcinoma cell line [11]. Cytotoxic activity has also been reported for a series of N-(thiophen-2-yl)benzamide derivatives employed to control the V600E BRAF kinase mutation [12]. N-acetyldinaline[4-(acetylamino)-N-(2-amino-phenyl)benzamide] has also demonstrated a

wide spectrum of antitumor activity in preclinical models [13, 14]. N-(2-Aminophenyl)-4-[N-(pyridine-3ylmethoxycarbonyl)aminomethyl]benzamide (MS275), a synthetic benzamide derivative, has been known for its proapoptotic properties, depending on tissue/cell type, doses, or incubation time [15]. Three benzamide derivatives of oxo-thiazolidinbenzamide have also been found to exhibit antitumor activity against Dalton's lymphoma ascites (DLA) cells [16].

A few studies have indicated that metal-based drugs show more cytotoxic activity against cancer cell lines compared to their ligands [17–19]. These effects have led to an increased interest in the preparation of these compounds and complexes, to study their pharmaceutical and medicinal properties [20–24]. Among the metal-based drugs that are used as anticancer agents, copper complexes have attracted more attention due to the role of copper as an essential element in human life [25, 26]. The series of R-heterocyclic Cu(II) thiosemicarbazonato complexes (Cu(TSC)Cl) have exhibited more cytotoxic activity against two breast cancer cell lines, SK-BR-3 and MCF-7, than their free ligands [27].

Moreover, copper complexes, including 2-oxo-1,2-dihydroquinoline-3-carbaldehyde(4′-methylbenzoyl)hydrazine, have shown higher cytotoxic activity against human cervical cancer cells (HeLa) and human laryngeal epithelial carcinoma cells (HEp-2) than their ligands; for example, the ligand (4′-methylbenzoyl)hydrazone (H2L) exhibited lower IC_{50} values of 127 ± 5 μM against HeLa cell line and 145 ± 4 μM against HEp-2 cell line compared to the respective IC_{50} values of 28.3 ± 1.6 and 9.3 ± 1.2 μM of its copper(II) complexes, square pyramidal complex $[Cu(H_2L)Cl_2]\cdot 2H_2O$ with copper(II) chloride and square planar complex $[Cu(HL)NO_3]\cdot DMF$ with copper(II) nitrate [28].

Considering the increasing importance of benzamide compounds and their copper complexes as anticancer agents, this study aimed to synthesize and characterize novel benzamide derivatives and their metal complexes with cytotoxic activity against different human cancer cell lines. For this purpose, three carbamothioylbenzamide derivatives were synthesized and used as starting materials. Reactions of the synthesized derivatives with copper(II) chloride yielded three new thiadiazolobenzamide derivatives and their copper(II) complexes. All these compounds were examined and screened by *in vitro* analysis for their cytotoxic activity to inhibit the proliferation of five human cancer cell lines: MDA-MB-231, SKNMC, LNCap, KB, and HEPG-2.

2. Experimental

2.1. General procedure

Benzoyl chloride, potassium thiocyanate, 2-aminopyridine, 4-methyl-2-aminopyridine, 6-methyl-2-aminopyridine, copper(II) chloride dehydrate, and all used solvents were supplied by Merck. All chemical compounds were used without further purification. A few experiments were performed using the microwave oven Samsung Trio, CE117ADV (230 V, 50 HZ). Melting points were determined by Electro Thermal IA 9000 Series. FT-IR spectra were obtained with a Nicolet 5SXC spectrometer, using KBr (4000–400 cm^{-1}) pellets. The ^{1}H and ^{13}C NMR spectra were recorded on a Bruker Advance 500 spectrometer at room temperature in acetone-d^6 and DMSO-d^6, using TMS as an internal reference. Elemental analysis of C, H, and N was performed on an Fligan Flash 1112 elemental analyzer. The quantity of Cu in the complexes was defined by the Varain Spectra 200-Rapid atomic absorption spectroscopy.

Diffraction data for crystals of carbamothioylbenzamide derivatives (compounds **2** and **3**), thiadiazolobenzamide derivatives (ligands **O1**, **O2**, and **O3**), and complexes **C2** and **C3** were collected on a Bruker AXS SMART diffractometer at room temperature using Mo Kα radiation (λ = 0.71073 Å) monochromatized by a graphite crystal. Data reduction was carried out using the Bruker AXS SAINT and SADABS packages [29]. The structure was solved by direct methods and refined by a full-matrix least-squares calculation using SHELX [30]. An empirical absorption correction (Ψ-scan) was applied. All non-hydrogen atoms were refined anisotropically. The positions of hydrogen atoms were calculated corresponding to their geometrical conditions and refined using a riding model. Isotropic displacement parameters of hydrogen atoms were derived from the parent atoms.

2.2. Synthesis and characterization of carbamothioylbenzamide derivatives: compounds 1, 2, and 3

Compounds **1** (*N*-(pyridine-2-ylcarbamothioyl)benzamide), **2** (*N*-(4-methylpyridine-2-ylcarbamothioyl)benzamide), and **3** (*N*-(6-methylpyridine-2-ylcarbamothioyl)benzamide) were prepared according to the reported protocol, which was modified in our laboratory [31]. According to the modified protocol, benzoyl chloride (0.5 mmol) and potassium thiocyanate (0.5 mmol) were mixed in acetonitrile (10 cm^3) at room temperature. The mixture was stirred for 30 min and 2-aminopyridine derivative (0.5 mmol) was gradually added. The mixture was warmed

to 50–60°C for 4–8 h, incubated at room temperature for 24 h, and finally filtered. The precipitate was purified by recrystallization from the solution of ethanol and acetone (1:1), and the potassium chloride that remained undissolved was separated.

Compounds **2** and **3** were also prepared using microwave as an energy source (**2**: 90 W, 5 min; **3**: 360 W, 10 min) and acetonitrile as a solvent. The ratio of reactants was the same as that in the modified reported protocol. Identification and characterization of synthesized compounds **1**, **2**, and **3** were conducted by melting point, elemental analysis, IR spectroscopy, ^{1}HNMR spectroscopy, ^{13}CNMR spectroscopy, and X-ray analysis (Scheme 1).

Compound 1: *N*-(pyridine-2-ylcarbamothioyl)benzamide

Light yellow powder, yield Reflux 40%, MP. 138–139ºC.

^{1}HNMR (acetone-d^6, 500 MHZ): δ 8.95 (s, 1H, H1), 7.28 (d, 1H, H2), 7.74 (s, 1H, H4), 8.46 (d, 2H, H9 and 13), 8.10 (dd, 2H, H10 and 12), 7.90 (t, 1H, H11), 13.36 (s, 1H, N2H), and 10.36 (s, 1H, N3H).

^{13}CNMR (acetone-d^6, 125 MHZ): 149.00 (C1), 121.76 (C2), 138.02 (C3), 115.86 (C4), 152.13 (C5), 178.16 (C6), 168.36 (C7), 133.76 (C8), 129.14 (C9 and 13), 128.68 (C10 and 12), and 132.66 (C11).

FTIR data (KBr, cm^{-1}): ν 3277m (NH), 2923w, 1703m, 1667s (C=O), 1557s (C=N+C=C(py)), 1524m, 1486m (C=N+C=C(py)), 1381s, 1350m (C=S), 1298s, 1248s (C=S), 1156m, 1061m (C–N), 847m (C=S), 753m, 712s, 694w (py), and 569w.

Elemental analysis calculated for $C_{14}H_{13}N_3OS$: C, 61.16%; H, 3.55%; N, 16.46%; Found: C, 61.04%; H, 4.27%; N, 16.89%.

Compound 2: *N*-(4-methylpyridineylcarbamothioyl)benzamide

Light yellow powder, yield MWI 63.5%, Reflux 42.2%, MP. 140–142ºC.

^{1}HNMR (acetone-d6, 500 MHZ): δ 2.29 (s, 3H, CH_3), 8.29 (s, 1H, H1), 7.10 (d, 1H, H2), 8.80 (s, 1H, H4), 8.08 (d, 2H, H9 and 13), 7.59 (dd, 2H, H10 and 12), 7.70 (t, 1H, H11), 13.36 (s, 1H, N2H), and 10.36 (s, 1H, N3H).

^{13}CNMR (acetone-d6, 125 MHZ): δ 21.33 (CH_3), 149.11 (C1), 123.18 (C2), 149.90 (C3), 116.80 (C4), 152.70 (C5), 177.86 (C6), 168.74 (C7), 134.21(C8), 129.61 (C9 and 13), 129.13 (C10 and 12), and 133.18 (C11).

FTIR data (KBr, cm^{-1}): ν 3213m (NH), 2923w, 1703m (C=O), 1675s, 1567s, 1524m (C=N+C=C(py)), 1486m (C=N+C=C(py)), 1381s, 1345m (C=S), 1298s, 1260s (C=S), 1156m (C–N), 1068m, 885m (C=S), 753m, 712s, 688w (py), and 569w.
Elemental analysis calculated for $C_{14}H_{13}N_3OS$: C, 61.97%; H, 4.83%; N, 15.49%; Found: C, 60.04%; H, 3.90%; N, 14.30%.

Compound 3: *N*-(6-methylPyridine-2-yl-carbamothioyl)benzamide

Yellow powder, yield MWI 53.8%, Reflux 70.4%, MP. 142–144ºC.
^{1}HNMR (acetone-d^6, 500 MHZ): δ 2.49 (s, 3H, CH_3), 7.14 (d, 1H, H2), 7.77 (s, 1H, H3), 8.76 (s, 1H, H4), 8.29 (d, 2H, H9 and 13), 7.60 (dd, 2H, H10 and 12), 7.71 (t, 1H, H11), 10.13 (s, 1H, N2H), and 13.29 (s, 1H, N3H).
^{13}CNMR (acetone-d^6, 125 MHZ): δ 23.55(CH_3), 151.39 (C1), 121.06 (C2), 138.29 (C3), 112.66 (C4), 158.05 (C5), 177.86 (C6), 168.25 (C7), 133.75 (C8), 129.13 (C9 and 13), 128.67 (C10 and 12), and 132.69 (C11).
FTIR data (KBr, cm^{-1}): ν 3192w (NH), 2930w, 1713s (C=O), 1610m, 1557s, 1529s (C=N+C=C(py)), 1493m (C=N+C=C(py)), 1443s, 1414m, 1380m, 1333s (C=S), 1239s (C=S), 1212m, 1176vs, 1195m, 1159s (C–N), 1084w, 1068m, 1023w, 999w, 969w, 899m (C=S), 793s, 747, 701s, 684m (py), 662s, and 516s.
Elemental analysis calculated for $C_{14}H_{13}N_3OS$: C, 61.97%; H, 4.83%; N, 15.49%, Found: C, 62.45%; H, 4.08%; N, 14.70%.

2.3. Synthesis and characterization of novel (1,2,4)thiadiazolo[2,3-a]pyridinebenzamide derivatives: ligands O1, O2, and O3

Copper(II) chloride (0.084 g, 0.5 mmol) in 3 cm^3 ethanol was added to each of the solutions of compounds **1**, **2**, and **3** (0.5 mmol) in 10 cm^3 acetone. The reaction was heated at 55°C and stirred for 5 h. Precipitates, obtained as the products of oxidative cyclization (ligands **O1**, **O2**, and **O3**), were filtered, and yellowish-orange or yellowish-green powders were separated. These precipitates were characterized by CHN and IR, ^{1}HNMR, and ^{13}CNMR spectroscopies (Scheme 1).

Scheme 1 Schematic of synthesis of **O1**, **O2**, **O3**, **C1**, **C2**, and **C3**

Ligand O1: *N*-(2H-[1,2,4]thiadiazolo[2,3-a]pyridine-2-ylidene)benzamide

Yellowish-white powder, yield 98%, MP 251°C.

^{1}HNMR (DMSO-d^6, 500 MHZ): δ 9.16 (d, 1H), 7.66 (dd, 1H), 7.49 (dd, 1H), 8.95 (d, 1H), 8.23 (d, 2H, H9 and H13), 7.57 (dd, 2H, H10 and H12), and 8.16 (t, 1H, H11).

^{13}CNMR (DMSO-d^6, 125 MHZ): δ 139.97 (C1), 118.85 (C2), 137.74 (C3), 117.85 (C4), 155.30 (C5), 173.34 (C6), 174.86 (C7), 133.14 (C8), 128.68 (C9 and C13), 128.72 (C10 and C12), and 131.16 (C11).

FTIR data (KBr, cm^{-1}): ν 3026w, 2825w, 1644s (C=O), 1624m (C=N), 1600m, 1578m (C=N), 1556s, 1529s (C=C+C=N(py)), 1468s (C=C+C=N(py)), 1310m, 1287s, 1253w, 1107m (C–N), 1089m, 1026w, 921m, 888m, 771m, 703s (C–S), and 662w (py).

Elemental analysis calculated for $C_{13}H_9N_3OS$: C, 61.16%; H, 3.55%; N, 16.46%, Found: C, 61.04%; H, 4.27%; N, 16.89%.

Ligand O2: *N*-(7-methyl-2H-[1,2,4]thiadiazolo[2,3-a]pyridine-2-ylidene)benzamide

Yellow powder, yield 99%, MP. 256ºC.

^{1}HNMR (DMSO-d^6, 500 MHZ): δ 2.45 (s, CH_3), 8.90 (s, 1H), 7.24 (d, 1H), 7.67 (s, 1H), 8.22 (d, 2H, H9 and H13), 7.54 (dd, 2H, H10 and H12), and 7.61 (t, 1H, H11).

^{13}CNMR (DMSO-d^6, 125 MHZ): δ 21.04 (CH_3), 151.41 (C1), 119.02 (C2), 133.29 (C3), 117.62 (C4), 155.56 (C5), 175.84 (C6), 176.69 (C7), 133.43 (C8), 128.58 (C9), 128.61 (C10), and 132.45 (C11).

FTIR data (KBr, cm^{-1}): ν 3025w, 2916w, 1662w (C=O), 1623m (C=N), 1617s, 1595m (C=N), 1543w, 1515s (C=C+C=N(py)), 1480s (C=C+C=N(py)), 1447s, 1430w, 1370s, 1327w, 1266s, 1237w, 1186m, 1146s (C–N), 1069w, 1025m, 897m, 859m, 813m, 791m, 722s (C–S), and 659w (py).

Elemental analysis calculated for $C_{14}H_{11}N_3OS$: C, 62.44%; H, 4.11%; N, 15.60%, Found: C, 62.97%; H, 3.90%; N, 16.09%.

Ligand O3: *N*-(5-methyl-2H-[1,2,4]thiadiazolo[2,3-a]pyridine-2-ylidene)benzamide

Yellow powder, yield 99%, MP. 253ºC.

^{1}HNMR (DMSO-d^6, 500 MHZ): δ 2.78 (s, CH_3), 7.27 (d, 1H), 7.59 (s, 1H), 7.71 (d, 1H), 8.21 (d, 2H, H9 and H13), 7.53 (dd, 2H, H10 and H12), and 8.01 (t, 1H, H11).

^{13}CNMR (DMSO-d^6, 125 MHZ): δ 19.76 (CH_3), 145.08 (C1), 115.62 (C2), 138.57 (C3), 116.64 (C4), 155.32 (C5), 174.58 (C6), 176.24 (C7), 132.90 (C8), 129.25 (C9), 128.23 (C10), and 132.10 (C11).

FTIR data (KBr, cm^{-1}): ν 3048w, 1650s (C=O), 1621s (C=N), 1588w, 1567s, 1561s (C=N), 1526s (C=C+C=N(py)), 1487w (C=C+C=N(py)), 1444m, 1389w, 1378s, 1329s, 1288m, 1277s, 1170m (C–N), 1065w, 905m, 796m, 721m (C–S), 710m, and 655w (py).

Elemental analysis calculated for $C_{14}H_{11}N_3OS$: C, 62.44%; H, 4.11%; N, 15.60%, Found: C, 61.97%; H, 4.83%; N, 15.23%.

2.4. Synthesis and characterization of complexes C1, C2, and C3

Complexes **C1**, **C2**, and **C3** were synthesized via the reaction of copper(II) chloride dihydrate and respective ligands **O1**, **O2**, and **O3**. Copper(II) chloride dihydrate (0.084 g, 0.5 mmol) in 5 cm^3 ethanol was added gradually to the solutions of ligands **O1** (0.128 g, 0.5 mmol), **O2** (0.135 g, 0.5 mmol), and **O3** (0.135 g, 0.5 mmol) in 8 cm^3 acetone. The mixtures were heated at 55°C and stirred for 18 h. The obtained mixture was filtered; after 5 days at room temperature, the complexes, in the form of jasper green crystals, could be isolated from the filtrate. The crystals were characterized by CHN and IR, ^{1}HNMR, and ^{13}CNMR spectroscopies; all these spectroscopic analyses indicated a common formula [Cu(**O**)$_2$Cl$_2$] for all obtained complexes (Scheme 1).

Complex C1:

dichlorobis(*N*-(2H-[1,2,4]thiadiazolo[2,3-a]pyridine-2ylidene)benzamide) copper(II)

Jasper green crystals, yield 54%.

^{1}HNMR (DMSO-d^6, 500 MHZ): δ 9.18 (d, 1H), 7.71 (dd, 1H), 7.47 (dd, 1H), 7.90 (d, 1H), 8.22 (d, 2H, H9 and 13), 7.56 (dd, 2H, H10 and 12), and 8.14 (t, 1H, H11).

^{13}CNMR (DMSO-d^6, 125 MHZ): δ 139.45 (C1), 117.26 (C2), 133.14 (C3), 117.12 (C4), 155.04 (C5), 172.33 (C6), 174.35 (C7), 134.32 (C8), 128.15 (C9 and C13), 128.10 (C10 and C12), and 131.02 (C11).

FT-IR data (KBr, cm^{-1}): ν 3062w, 2835w, 1653s (C=O), 1621m (C=N), 1610m, 1588m (C=N), 1566s, 1523s (C=C+C=N(py)), 1481s (C=C+C=N(py)), 1310m, 1287s, 1255w, 1166m (C–N), 1089m, 1026w, 921m, 868m, 751m, 719s (C–S), and 674w (py).

Elemental analysis calculated for $C_{28}H_{22}Cl_2CuN_6O_2S_2$: C, 52.09%; H, 3.43%; N, 13.03%; Cu, 9.85% Found: C, 51.67%; H, 4.20%; N, 13.56%; Cu, 9.40%.

Complex C2:

dichlorobis(*N*-(7-methyl-2H-[1,2,4]thiadiazolo[2,3-a]pyridine-2ylidene)benzamide) copper(II)

Jasper green crystals, yield 56%.
^{1}HNMR (DMSO-d^6, 500 MHZ): δ 2.49 (s, CH_3), 8.91 (d, 1H, H1), 7.24 (d, 1H, H2), 7.66 (s, 1H, H4), 8.22 (d, 2H, H9 and 13), 7.54 (dd, 2H, H10 and 12), and 7.60 (t, 1H, H11).
^{13}CNMR (DMSO-d^6, 125 MHZ): δ 20.85 (CH_3), 151.18 (C1), 118.81 (C2), 133.24 (C3), 117.4 2 (C4), 155.48 (C5), 175.05 (C6), 176.66 (C7), 133.08 (C8), 128.16 (C9 and 13), 128.13 (C10 and 12), and 132.24 (C11).
FT-IR data (KBr, cm^{-1}): ν 3035w, 2921w, 1659s (C=O), 1628s (C=N), 1590m (C=N), 1523s (C=C+C=N(py)), 1481m (C=C+C=N(py)), 1444s, 1365sm, 1329m, 1267m, 1237w, 1159w (C–N), 1118w, 1027m, 897w, 852w, 805s, 717s (C–S), 677m (py), 584m, 522w, 457w, and 433vw.
Elemental analysis calculated for $C_{28}H_{22}Cl_2CuN_6O_2S_2$: C, 49.96%; H, 3.29%; N, 12.48%; Cu, 9.40% Found: C, 48.80%; H, 4.50%; N, 11.98%; Cu, 10.04%.

Complex C3:

dichlorobis(*N*-(5-methyl-2H-[[1,2,4]thiadiazolo[2,3-a]pyridine-2ylidene)benzamide) copper(II)

Jasper green crystals, yield 57%.
^{1}HNMR (DMSO-d^6, 500 MHZ): δ 2.80 (s, CH_3), 7.35 (d, 1H, H2), 7.63 (dd, 1H, H3), 7.81 (d, 1H, H4), 8.20 (d, 2H, H9 and 13), 7.54 (dd, 2H, H10 and 12), and 8.07 (t, 1H, H11).
^{13}CNMR (DMSO-d^6, 125 MHZ): δ 19.62 (CH_3), 145.29 (C1), 117.20 (C2), 131.48 (C3), 115.71(C4), 154.78 (C5), 172.18 (C6), 174.60 (C7), 138.99 (C8), 128.13 (C9 and 13), 128.16 (C10 and 12), and 132.46 (C11).
FT-IR data (KBr, cm^{-1}): ν 3006w, 2923w, 1652m (C=O), 1621m (C=N), 1594m (C=N), 1540m (C=C+C=N(py)), 1489m (C=C+C=N(py)), 1445s, 1378s, 1332s, 1280m, 1240m, 1169m (C–N), 1098w, 1064m, 1009vw, 906m, 797m, 723s (C–S), 680m (py), 542vw, and 478vw.

Elemental analysis calculated for $C_{28}H_{22}Cl_2CuN_6O_2S_2$: C, 49.96%; H, 3.29%; N, 12.48%; Cu, 9.40%, Found: C, 49.05%; H, 4.30%; N, 13.08%; Cu, 8.96%.

For single-crystal X-ray diffraction experiments, suitable crystals of compounds **2** and **3** were obtained by recrystallization of their ethanol and acetone (1:1) solutions. Suitable crystals of ligands **O1**, **O2**, and **O3** were obtained by recrystallization of their methanol and acetonitrile (1:1) solutions. The isolated jasper green crystals of complexes **C2** and **C3** were used for X-ray diffraction experiments (Table 1).

2.5. Cell culture and *in vitro* cytotoxicity assay

Five human cell lines, breast cancer cell line MDA-MB-231, neuroblastoma cell line SK-N-MC, prostate adenocarcinoma cell line LNCap, nasopharyngeal epidermoid carcinoma cell line KB, and liver cancer cell line HEPG-2 were obtained from National Cell Bank of Iran (NCBI, Iran). The cells were grown in an RPMI-1640 medium supplemented with 10% heat-inactivated fetal calf serum (from GibcoeBRL, UK), 100 mg/cm^3 streptomycin, and 100 U/cm^3 penicillin at 37°C/95% rh/5% CO_2. *In vitro* cytotoxic activities of the test compounds **1**, **2**, **3**, **O1**, **O2**, **O3**, **C1**, **C2**, and **C3** were investigated in comparison to standard chemotherapy drugs doxorubicin (DOX) and etoposide, using a modified MTT-dye reduction assay [32]. Briefly, cultures in the exponential growth phase were trypsinized and diluted in a complete growth medium to a total cell count of 5×10^4 cells/cm^3. Then 195×10^{-3} cm^3 of suspension was added to the wells of a sterile 96-well plate (NUNC, Denmark) and allowed to attach for overnight. After plating, 5×10^{-3} cm^3 of a serial concentration of every compound was added. The plates were incubated for 48 h. After incubation, 200×10^{-3} cm^3 of 0.5 mg/cm^3 solution of MTT (Sigma-Aldrich, Steinheim, Germany) was added to each well and the plate was again incubated for 4 h. Then the culture medium was replaced with 100×10^{-3} cm^3 of DMSO, and the absorbance was measured at 492 nm. Each experiment was carried out in triplicate for each concentration. DOX and etoposide were used as positive controls for cytotoxicity, and the tumor cells cultured in 200×10^{-3} cm^3 of complete medium were applied as controls for cell viability. For each compound, the concentration causing 50% inhibition in cell growth (IC_{50} value) was calculated from the concentration response curves using regression analysis.

3. Results and discussion

3.1. Spectroscopic studies

Infrared spectroscopy was used to study the solid-state properties of all synthesized compounds, ligands, and complexes. No absorption bands characteristic of the NH groups were observed for ligands **O1**, **O2**, and **O3**, because compounds **1**, **2**, and **3** were oxidized by copper(II) and lost two hydrogen atoms of the NH groups. In addition, complexes **C1**, **C2**, and **C3**, including the coordinated ligands, did not indicate any absorption bands for the NH groups. During oxidation, the sulfur atom was joined to the nitrogen atom of the pyridine ring, forming a five-membered ring.

The presence of the C=N bond, after oxidation and cyclization, was confirmed by the absorption bands at 1624 and 1578 cm^{-1} (**O1**), 1632 and 1592 cm^{-1} (**O2**), 1621 and 1561 cm^{-1} (**O3**), 1630 and 1588 cm^{-1} (**C1**), 1628 and 1590 cm^{-1} (**C2**), and 1621 and 1594 cm^{-1} (**C3**) [33].

The ^{1}H NMR spectroscopy characterized the structural properties of sample in solution. The chemical shifts of 13.36 and 10.36 ppm (**1**), 13.36 and 10.36 ppm (**2**) and 10.13 and 13.29 ppm (**3**) correspond to the hydrogen atoms in NH bonds. Differences in the chemical shifts for each compound revealed the extent of intramolecular hydrogen bonding in N2H, N2H and N3H (13.36, 13.36, and 13.29 ppm), which caused the movement of resonances to the down field in compounds **1**, **2** and **3** [34–36]. Absence of resonances above 10 ppm in **O1**, **O2**, **O3**, **C1**, **C2**, and **C3** confirmed the removal of hydrogen atoms from NH groups [34, 37–39].

The data of ^{13}C NMR spectra showed no significant differences in the chemical shifts of compounds **1**, **2**, and **3**; ligands **O1**, **O2**, and **O3**, and complexes **C1**, **C2**, and **C3**. The position of the methyl group had no effect on the chemical shift. During oxidative cyclization, the conversion of C=S bond to C–S bond in **O1**, **O2**, **O3**, **C1**, **C2**, and **C3** decreased the chemical shift of carbon to up field and increased the resonance of C=O bond to down field [40].

3.2. Crystal structure

Relevant crystallographic information of **O1**, **O2**, **O3**, **C1**, **C2** and **C3** has been summarized in Table 1.

Table 1 Crystallographic refinement data for compounds **2** and **3**, ligands **O1**, **O2**, and **O3** and complexes **C2**, and **C3**

	2	**3**	**O1**	**O2**	**O3**	**C2**	**C3**
Empirical formula	$C_{14}H_{13}N_3OS$	$C_{14}H_{13}N_3OS$	$C_{13}H_9N_3OS$	$C_{14}H_{11}N_3OS$	$C_{14}H_{11}N_3OS$	$C_{28}H_{22}Cl_2CuN_6O_2S_2$	$C_{28}H_{22}Cl_2CuN_6O_2S_2$
Formula weight	271.33	271.33	255.29	269.32	269.32	673.07	673.07
T (K)	294 (2)	294(2)	273(2)	273(2)	296(2)	294(2)	294 (2)
Wavelengths (Å)	0.71073	0.71073	0.71073	0.71073	0.71073	0.71073	0.71073
Crystal system	Monoclinic	Monoclinic	Monoclinic	Monoclinic	Monoclinic	Triclinic	Monoclinic
Space group	$P2_1/c$	$P2_1/n$	$P2_1/c$	$P2_1/n$	$P2_1/c$	P-1	$P2_1/n$
a (Å)	12.018(4)	7.201(3)	6.255(3)	11.678(6)	12.7107(7)	8.158(5)	13.947(4)
b (Å)	5.2813(16)	18.487(8)	18.109(7)	3.995(2)	18.0290(9)	8.426(5)	14.750(5)
c (Å)	21.723(6)	10.441(5)	10.221(4)	26.939(15)	11.5181(6)	11.183(6)	13.894(4)
α (º)	-	-	-	-	-	78.716(8)	-
β (º)	97.502(4)	108.926(7)	95.525(6)	98.965(9)	101.980(3)	76.857(8)	98.561 (5)
γ (º)	-	-	-	-	-	71.514(8)	-
V ($Å^3$)	1367.0 (7)	1314.9(10)	1152.4(8)	1241.4(12)	2582.0(2)	703.6(7)	2827.1(14)
Z	4	4	4	4	8	1	4
D (g cm^{-3})	1.318	1.371	1.471	1.366	1.386	1.589	1.579
μ (mm^{-1})	0.232	0.241	0.270	0.251	0.245	1.154	1.149
Rint	0.0589	0.0507	0.0462	0.0507	0.0824	0.0449	0.0582
Completeness to θ (%)	95.2 (θ=30.36°)	99.6 (θ =26.45°)	99.4 (θ=27.56°)	99.3 (θ =23.94°)	99.2 (θ =24.76°)	97.8 (θ =29.49°)	99.7 (θ =28.25°)
Final R indices [I > 2σ(I)]	R1 = 0.0417, wR2 = 0.1051	R1= 0.0384, wR2 = 0.0892	R1 = 0.0361, wR2 = 0.0735	R1 = 0.0502, wR2 = 0.1286	R1 = 0.0385, w R1 = 0.0972	R1 = 0.0406, w R1 = 0.0973	R1 = 0.0420, w R1 = 0.0945
R indices (all data)	R1 = 0.1109, wR2 = 0.1231	R1= 0.0681, wR2 = 0.0969	R1 = 0.0845, wR2 = 0.0833	R1 = 0.0767, wR2 = 0.1604	R1= 0.0607, wR2 = 0.1060	R1 = 0.0568, wR2 = 0.0973	R1 = 0.0813, wR2 = 0.1008
CCDC †	714500	714501	711636	713327	962672	714502	714503

† These data can be obtained free of charge via http:// www.ccdc.cam.ac.uk/conts/retrieving.html or from the Cambridge Crystallographic Data Centre, 12 Union Road, Cambridge CB2 1EZ, UK; fax: (+44) 1223-336-033; or e-mail: deposit@ccdc.cam.ac.uk.

Compounds 2 and 3

The similar bond lengths and angles in compounds **2** and **3** (Table 2) indicated that the position of the substituted alkyl group on the pyridine ring has no effect on bond lengths and angles (Figs. 1 and 2) [36]. The crystal structure of previously reported compound **1** (Supplemental materials, Fig. S1) [31] is similar to that of compound **2** (Fig. 1).

Fig. 1 Molecular structure of compound **2** (30% probability level)

Fig. 2 Molecular structure of compound **3** (30% probability level)

The strong intramolecular hydrogen bonding, N2–H2---O1 (2.597 Å and 143.3°), in compound **2** shifted the resonance of the hydrogen to down field. However, the chemical shift in compound **3** is caused by the strong intramolecular hydrogen bonding, N3–H3---N1 (2.664 Å and 140.3°). In the unit cell of compound **2**, two weak intermolecular hydrogen bonds (N3–H3---S1) connect two molecules together and form a centrosymmetric dimer in the solid state (Fig. 3). In contrast, in the unit cell of compound **3**, three weak intermolecular hydrogen bonds (N2–H2---S1 and C2–H2---O1) bind the molecules (Fig. 4).

Fig. 3 View of the unit cell of compound **2** with hydrogen bonding
(1: x, y, z; 2: – x, ½ + y, ½ – z; 3: – x, – y, – z; 4: x, ½ – y, ½ + z)

Fig. 4 View of the unit cell of compound **3** with hydrogen bonding
(1: x, y, z; 2: ½ – x, ½ + y, ½ – z; 3: – x, – y, – z; 4: ½ + x, ½ – y, ½ + z)

Table 2 Selected bond lengths (Å) and angles (º) in compounds **1**, **2**, and **3**

bond length (Å)	1[31]	2	3	bond angle (º)	1[31]	2	3
N1-C5	1.325(5)	1.329(2)	1.330(2)	C1-N1-C5	117.0(4)	116.13(18)	117.78(15)
N2-C5	1.417(4)	1.403(2)	1.407(2)	N1-C5-N2	109.9(3)	109.76(16)	118.45(15)
N2-C6	1.329(4)	1.336(2)	1.358(2)	C5-N2-C6	114.7(3)	132.88(15)	131.70(14)
N3-C6	1.382(4)	1.383(2)	1.367(2)	N2-C6-S1	126.8(3)	127.22(14)	118.98(13)
N3-C7	1.388(4)	1.382(2)	1.392(2)	N3-C6-S1	118.6(3)	118.60(12)	126.21(13)
S1-C6	1.658(3)	1.653 (2)	1.662 (2)	N2-C6-N3	114.7(3)	114.18(15)	114.78(14)
O1-C7	1.220(4)	1.220(2)	1.201(2)	C6-N3-C7	128.5(3)	129.06(15)	128.32(15)
C7-C8	1.470(5)	1.476(3)	1.491(2)	O1-C7-N3	121.5(3)	121.35(18)	122.68(16)
		-	-	O1-C7-C8	121.7(3)	121.48(16)	122.23(16)
		-	-	N3-C7-C8	116.8(3)	117.17(16)	115.08(15)

Ligands O1, O2, and O3

Oxidative cyclization of compounds **1**, **2**, and **3** changed their bond lengths and resulted in the formation of N–S bond (N of pyridine ring) in ligands **O1**, **O2**, and **O3**. The N–S bond and changed bond lengths were confirmed by measuring the bond lengths and angles of ligands **O1** (Supplemental materials, Fig. S2), **O2**, and **O3** (Figs. 5 and 6, Table 3). The alkyl group on the

pyridine ring had no effect on the bond lengths and angles. The planar structure of ligands caused by conjugated double bonds and the nonbonding electron pair of the nitrogen atom (N3) was confirmed by the torsion angles (Supplemental materials, Table S1). The obtained data indicated. The obtained data indicated that ligands **O1** and **O2** have similar structures.

Fig. 5 Molecular structure of ligand **O2** (30% probability level)

Fig. 6 Molecular structure of ligand **O3** (30% probability level)

Table 3 Selected bond length (Å) and angle (º) in ligands **O1**, **O2**, and **O3**

bond length (Å)	O1	O2	O3	bond angle(º)	O1	O2	O3
N1-S1	1.7623(16)	1.768(3)	1.7736(17) [c]	C1-N1-C5	122.85(17)	121.0(3)	122.57(18) [b]
N1-C5	1.357(2)	1.267(4)	1.365(3) [b]	C5-N1-S1	111.54(13)	112.3(2)	111.56(14) [b]
N2-C5	1.352(2)	1.346(4)	1.347(3) [a]	N1-C5-N2	115.48(17)	114.7(3)	115.34(18) [b]
N2-C6	1.311(2)	1.333(4)	1.319(3) [c]	N1-S1-C6	85.96(9)	86.07(15)	85.69(9)
S1-C6	1.7637(19)	1.776(3)	1.762(2) [c]	C5-N2-C6	110.90(16)	112.2(3)	110.98(19)
N3-C6	1.339(2)	1.325(4)	1.348(3) [c]	N2-C6-S1	116.11(15)	114.8(3)	116.42(16)
N3-C7	1.338(2)	1.346(4)	1.345(3) [d]	N3-C6-S1	120.83(15)	120.6(2)	120.78(16)
O1-C7	1.264(2)	1.267(4)	1.259(3) [d]	N2-C6-N3	123.05(17)	124.6(3)	122.8(2)
S1-O1	2.1678(15)	2.156(3)	2.141(2)	C6-N3-C7	112.52(16)	113.0(3)	113.39(19)
				O1-C7-N3	122.48(19)	121.7(3)	122.4(2)
				O1-C7-C8	119.84(17)	120.2(3)	120.8(2)
				N3-C7-C8	117.67(17)	118.1(3)	116.8(2)

[a] First molecule in the ortep **O3**
[b] C1 in **O3** = C5 in **O1** and **O2**; C13 in **O3** = C5 in **O1** and **O2**
[c] C2 in **O3** = C6 in **O1** and **O2**
[d] C3 in **O3** = C7 in **O1** and **O2**

In the unit cell of ligand **O1**, strong intramolecular interactions exist between sulfur and oxygen atoms (S1–O1, 2.168 Å), whereas weak intermolecular interactions exist between sulfur and carbon atoms (S1–C7, Å 3.445 Å). Several weak intermolecular hydrogen interactions (C1–H1---O1, 3.408 Å; C4–H4---N2, 3.466 Å; and C11–H11---N4, 3.363 Å) connect the molecules to each other and form a centrosymmetric crystal lattice (Supplemental materials, Fig. S3).

In the unit cell of ligand **O2**, the sulfur and oxygen atoms (2.156 Å) are connected by strong intramolecular bonding. The binding of two molecules over intermolecular hydrogen bonding

creates a centrosymmetric dimer (C1–H1---O1, 3.331 Å). Each molecule of dimers is connected again to the third molecule of other dimers by intermolecular hydrogen bonding (C4–H4---N2, 3.367 Å) (Fig. 7).

The obtained data indicated that the unit cell of ligand **O1** is similar to that of ligand **O2**.

Fig. 7 Unit cell of ligand **O2** with hydrogen bonding
(1: x, y, z; 2: ½–x, ½ +y, ½ – z; 3: – x, – y, – z; 4: ½ + x, ½ – y, ½ + z)

Strong intramolecular S---O bonding exists among different molecules in the unit cell of ligand **O3** (S1---O1, 2.210 Å and S2---O2, 2.140 Å) (Fig. 8). In addition, π–π weak interactions (3.625 Å in ligand **O1**, 3.995 Å in ligand **O2**, and 3.640 Å in ligand **O3**) are observed between two phenyl rings or between a phenyl and a pyridine ring.

Fig. 8 Unit cell of ligand **O3** with hydrogen bonding
(1: x, y, z; 2: – x, y + ½, ½ – z; 3: – x, – y, – z; 4: x, ½ – y, z + ½)

Ligands **O1**, **O2**, and **O3**, derivatives of [1,2,4]thiadiazolo[2,3-a]pyridine benzamide, reported in our work are the first benzamide derivatives that could be produced by oxidative cyclization reaction of *N*-(pyridine-2-ylcarbamothioyl)benzamide compounds using copper(II) ion as an oxidant. Planar ligands with structures similar to those of ligands **O1, O2**, and **O3** have not yet been reported in the literature.

The already published compounds containing [1,2,4]thiadiazolo[2,3-a]pyridine, which were produced by oxidative cyclization reaction of *N*-pyridyl-thioureas, are neither a benzamide derivative nor similar to our ligands **O1, O2**, and **O3** [41, 42].

Although 2,5-disubstituted oxazoles [43] and furoxan [44] have been reported to be produced by oxidative cyclization using copper(II) ion as an oxidant, contrary to our products, they are not able to react as ligands and cannot connect to copper ion to form complexes.

As reported by Che et al. [38, 45], the reaction of *N*-(pyridine-2-ylcarbamothioyl)benzamide (compound **1**) with copper (II) ion resulted in the formation of a polymeric tetrahedral complex directly, whereas in our study, this reaction produced the ligand **O1** in addition to complex **C1.** The ligand **O1** could be isolated and was tested for its cytotoxicity effect.

Complexes C2 and C3

Connection of ligands **O2** and **O3** to the copper(II) ion via their nitrogen atoms resulted in the formation of complexes **C2** and **C3** [46]. In both complexes, each copper ion with a coordination number of four was surrounded by two chloride ions and two ligands. Bond angles of about 90° with very small distortion resulted in the formation of a square planar structure around the copper ion. The bond lengths and angles around the central ion were similar in both **C2** and **C3** complexes (Figs. 9 and 10, Table 4; for more detailed information: Supplemental materials Table S2).

Fig. 9 Molecular structure of complex **C2** (30% probability level)

Fig. 10 Molecular structure of complex **C3** (30% probability level)

Table 4 Selected bond length (Å) and angle (º) in complexes **C2** and **C3**

bond length (Å)	C2	C3	bond angle (º)	C2	C3
Cu1-N2	1.988(2)	1.990(2)	N2-Cu1-N2#1/2B	180.0	168.33(9)
Cu1-N2#1/2B	1.988(2)	1.996(2)	N2-Cu1-Cl1	91.10(6)	91.92(7)
Cu1-Cl1	2.2637(14)	2.2356(10)	N2#1/2B-Cu1-Cl1	88.90(6)	91.37(7)
Cu1-Cl1#1/Cl2	2.2637(14)	2.2544(10)	N2-Cu1-Cl1#1/Cl2	88.90(6)	89.74(7)
S1-C6	1.754(2)	1.747(3)	N2#1/2B-Cu1-Cl1#1	91.10(6)	88.55(7)
S1-N1	1.795(2)	1.809(2)	Cl1-Cu1-Cl1#1/Cl2	180.0	171.94(4)
S1-O1	2.124(2)	2.076(2)	C6-S1-N1	85.53(10)	85.60(13)
N1-C5	1.361(3)	1.353(3)	C6-S1-O1	79.71(9)	80.43(12)
N1-C1	1.364(3)	1.368(3)	N1-S1-O1	165.22(7)	165.97(10)
N2-C6	1.333(3)	1.331(3)	C7-O1-S1	105.68(15)	106.36(18)
N2-C5	1.362(3)	1.363(3)	C5-N1-C1	121.4(2)	122.6(3)
N3-C6	1.328(3)	1.331(3)	C5-N1-S1	112.92(14)	112.13(19)
N3-C7	1.345(3)	1.344(3)	C1-N1-S1	125.63(15)	125.2(2)
			C6-N2-C5	112.73(18)	112.4(2)
			C6-N2-Cu1	117.29(14)	120.98(19)
			C5-N2-Cu1	129.87(15)	126.64(19)
			C6-N3-C7	111.69(19)	110.8(2)
			C2-C1-N1	119.4(2)	117.5(3)

The unit cell of complex **C2** has a triclinic crystal system, with z=1 and space group P-1. In this unit cell, weak π–π interactions between the phenyl rings (average 3.858 Å) of two complexes led to the formation of the crystal lattice (Fig. 11).

Fig. 11 π-π interaction between phenyl rings of two **C2** complexes
(1: x, y, z; 2: x, – y, –z)

The unit cell of complex **C3** has a monoclinic crystal system, with z=4 and space group $P2_1/n$. Two medium intramolecular hydrogen bonding, C14–H14A---S1 (3.104Å) and C14B–H14D---S1B (3.093Å), were observed in complex **C3** (Fig. 12).

Fig. 12 Unit cell of complex **C3** with hydrogen bonding
(1: x, y, z; 2: – x, ½ + y, ½ – z; 3: – x, – y, – z; 4: x, ½ + y, ½ – z)

Complexes **C2** and **C3** are characterized by large monodentate ligands and a stable square planar structure.

The most reported copper(II) ion complexes have a tetrahedral, square bipyramidal, or octahedral geometry [47, 48, 49]. Copper(II) ion complexes having a square planar structure have rarely been reported; most of these complexes are generated by the binding of bi- or more dentate ligands to copper(II) ion [50–54]. The complex $[Cu(C_6H_6N_3S_2)_2]$ with a square planar structure was reported to be formed by the binding of the bidentate ligand thiophene-2-carbaldehydethiosemicarbazone, to copper(II) ion [52] and the square planar complex [Cu(N-(2-methylpyridyl)benzenesulfonylamidate)$_2$] by the binding of the bidentate ligand N-(2-methylpyridyl)benzenesulfonylaide to the copper (II) ion [53].

Formation of a square planar structure through binding of monodentate ligands to the copper(II) ion has rarely been possible. The square planar structure of the complex [Cu(2-amino-5-bromopyridine)$_2$$(Cl)_2$], as reported by Ahmadi et al. [55], was formed by the binding of 2-amino-5-bromopyridine, a monodentate ligand, to copper(II) chloride. In complexes **C2** and **C3**, two large monodentate ligands were coordinated to copper(II) ion and a stable square planar structure, with a trans geometric configuration, was formed. As shown in Scheme 2, the core structure of monodentate ligands **O1**, **O2**, and **O3** is more complex than the monodentate ligand reported by Ahmad et al. The large scale of the monodentate ligands, their planar surface and the position of the cycles in them protect the square planar structure of complexes **C2** and **C3** against reactions with other ligands or solvent molecules and the copper–copper interaction. This leads to the excellent stability of the novel square planar structure of complexes **C2** and **C3**.

Scheme 2: Comparison of monodentate ligand reported by Ahmadi et al. to monodentate ligands **O1**, **O2**, and **O3**

3.3 *In vitro* cytotoxicity studies

The cytotoxic activity of compounds **1**, **2**, and **3**; ligands **O1**, **O2**, and **O3**; and complexes **C1**, **C2**, and **C3** against MDA-MB-231, SK-N-MC, LNCap, KB, and HEPG-2 human cancer cell lines were determined compared to references DOX and etoposide. Etoposide and DOX are standard chemotherapy drugs that have widely been used to treat different types of cancers, such as neuroblastoma, soft tissue and bone sarcomas, breast carcinoma, ovarian carcinoma, lung cancer, thyroid carcinoma, and gastric carcinoma [56, 57]. Since no benzamide-based copper(II) complex with an anticancer activity was available commercially, etoposide and DOX were used as positive references. Although compounds **1**, **2**, **3** did not exhibit any cytotoxic activity, such activity was demonstrated by ligands **O1**, **O2**, and **O3** and complexes **C1**, **C2**, and **C3**.

The IC_{50} values of ligands **O1**, **O2**, and **O3** and complexes **C1**, **C2**, and **C3** for all five cancer cell lines are shown in Figures 13–17. IC_{50} values of all ligands and complexes against all used cell lines are presented in Figure 18.

Fig. 13 IC_{50} values of **O1**, **O2**, **O3**, **C1**, **C2**, and **C3** against breast cancer cell line MDA-MB-231(SD = ± 2.00 %)

Fig. 14 IC_{50} values of **O1**, **O2**, **O3**, **C1**, **C2**, and **C3** against neuroblastoma cell line SK-N-MC (SD = ± 3.00 %)

Fig.15 IC_{50} values of **O1**, **O2**, **O3**, **C1**, **C2**, and **C3** against prostate adenocarcinoma cell line LNCap (SD = ± 3.00 %)

Fig. 16 IC_{50} values of **O1**, **O2**, **O3**, **C1**, **C2**, and **C3** against nasopharyngeal epidermoid carcinoma cell line KB (SD = ± 3.70 %)

Fig. 17 IC_{50} values of **O1**, **O2**, **O3**, **C1**, **C2**, and **C3** against liver cancer cell line HEPG-2 (SD = ± 1.70 %)

Fig. 18 Comparison of IC_{50} values of **O1**, **O2**, **O3**, **C1**, **C2**, and **C3** againts human cancer cell lines; ‖ MDA-MB-231, \\ SK-N-MC, ═ LNCap, ▓ KB, ▒ HEPG-2

The complexes showed higher cytotoxic activities than the ligands. This could be attributed to the presence of two ligands and the copper ion in each complex that synergistically increased the cytotoxicity [20, 28].

Compared to the other ligands and complexes, complex **C2** showed the lowest IC_{50} value and the highest cytotoxicity against all used cell lines, with the exception of the breast cancer cell

line MDA-MB-231. This complex with an IC_{50} value of 3.44 ± 0.01 μM showed the most significant inhibitory effect on the growth of the prostate adenocarcinoma cell line LNCap. The inhibition effect was comparable to that of the reference standard DOX and significantly stronger than that of etoposide. In addition, ligand **O2** as a part of complex **C2** showed a lower IC_{50} value and higher cytotoxicity against LNCap, KB, and HEPG-2 human cancer cell lines than the other ligands. This could be due to the different position of the methyl group in this ligand from that in the other ligands.

Complex **C3** with an IC_{50} value of 5.46 ± 0.66 μM showed the highest cytotoxic activity against the breast cancer cell line MDA-MB-2. The inhibition effect of this complex was approximately six times higher than that of the reference standard etoposide.

Some benzamide derivatives have been shown to possess cytotoxic activity. Different kinds of benzamide derivatives (**A** [3], **B** [9], and **C** [11]) showing cytotoxic activity against the breast cancer cell line MCF7 have been reported. Their IC_{50} values, ranging from 27.2 ± 7.1 to >100 μM, are as follows: **A**, N-(2-{4-[(3,7-dimethylocta-2,6-dien-1-yl)oxy]phenyl}ethyl)benzamide (IC_{50} 80.6 ± 4.0 μM) and N-(2-{4-[(3,7-dimethyl-4-acethyl-octa-2,6-dien-1-yl)oxy]phenyl}ethyl)benzamide (IC_{50} > 100 μM); **B**, N-benzyl-2-(2-cyano-3-(3,4-dimethoxyphenyl)acrylamido)benzamide (IC_{50} 9.90 μg/mL) and 2-(2-cyano-3-(3,4-dimethoxyphenyl)-acrylamido)-N-(2-hydroxyethyl)benzamide (IC_{50} 7.95 μg/mL); and **C**, 4-(5-fluoro-2-oxoindolin-3-ylideneamino)benzamide (IC_{50} > 100 μM), 4-(2-oxo-5-(trifluoromethoxy)indolin-3-ylideneamino)benzamide (IC_{50} 27.2 ± 7.1 μM), and 4-(5, 7-dichloro-2-oxoindolin-3-ylideneamino)benzamide (IC_{50} 65.86 ± 8.1 μM). The cytotoxic activity of our ligands **O1**, **O2**, and **O3** against the breast cancer cell line MDA-MB-231 was in a range of 13.92 ± 1.15 to 17.46 ± 0.58 μM (**O1**, IC_{50} 17.46 ± 0.58 μM; **O2**, IC_{50} 20.10 ± 4.93 μM; and **O3**, IC_{50} 13.92 ± 1.15 μM).

For the ligand H2PDIMAla and its complex $[Cu_2(dpq)_2(PDIMAla)(H_2O)_2](ClO_4)_2CH_3OH$, the IC_{50} values have been reported to be >160 and 2.7 μM, respectively, against the human prostate cancer cell line PC3 [25]. The IC_{50} values of complex **C2** and its ligand **O2**, which showed the highest cytotoxic activity against the human prostate cancer cell line PC3, were about 3.44 ± 0.01 and 12.21 ± 2.56 μM, respectively.

Conclusion

The reaction of 2-amino pyridine derivatives, potassium thiocyanate, and benzoyl chloride in one pot produced the following *N*-(pyridine-2-ylcarbamothioyl)benzamide derivatives: *N*-(pyridine-2-ylcarbamothioyl)benzamide, *N*-(4-methylpyridine-2-ylcarbamothioyl)benzamide, and *N*-(6-methylpyridine-2-ylcarbamothioyl)benzamide. Oxidation of the obtained derivatives using copper(II) chloride as an oxidant resulted in the removal of two hydrogen atoms, cyclization of the compounds, and finally, formation of three new *N*-(2H-[1,2,4]thiadiazolo[2,3-a]pyridine-2-ylidene)benzamide derivatives with planar structure: *N*-(2H-[1,2,4]thiadiazolo[2,3-a]pyridine-2-ylidene)benzamide, *N*-(7-methyl-2H [1,2,4]thiadiazolo[2,3-a]pyridine-2-ylidene)benzamide, and *N*-(5-methyl-2H [1,2,4]thiadiazolo[2,3-a]pyridine-2-ylidene)benzamide.

These planar ligands were coordinated to copper(II) ion, and three new complexes **C1**, **C2**, and **C3**, each consisting of two large monodentate ligands and two chlorine anions, were synthesized. These new complexes were neutral, having a rare square planar geometry around the copper ion. Due to the planar surface and the large scale of the monodentate ligands, the square planar structures of complexes **C1**, **C2**, and **C3** are well protected and very stable.

All obtained compounds, ligands, and complexes were subjected to an *in vitro* analysis using an MTT-based assay to define their cytotoxic activity against MDA-MB-231, SK-N-MC, LNCap, KB, and HEPG-2 human cancer cell lines.
N-(pyridine-2-yl-carbamothioyl)benzamide derivatives did not exhibit any cytotoxic activity. Significant cytotoxic activity could be observed by ligands **O1**, **O2**, and **O3** and complexes **C1**, **C2**, and **C3**. The complexes exhibited higher cytotoxic activities in comparison to the ligands.

Complex **C2** showed the highest cytotoxic activity against all used cell lines, with the exception of the breast cancer cell line MDA-MB-231. Ligand **O2** as a part of complex **C2** also showed a higher cytotoxic activity against the most analyzed cancer cell lines than the other ligands. Complex **C2**, with an IC_{50} value of 3.44 ± 0.01 μM, showed a significantly stronger inhibitory effect on the growth of the prostate adenocarcinoma cell line LNCap than the reference standard etoposide. The cytotoxic activity against the breast cancer cell line MDA-MB-2 of complex **C3** was about six times higher than that of the reference standard.

The straightforward and simple synthesis process, a stable square planar structure, and high cytotoxic activities of our compounds make these suitable candidates for anticancer therapy. Especially, complexes **C3** and **C2** with very high cytotoxic activities against the breast cancer

cell line MDA-MB-2 and prostate adenocarcinoma cell line LNCap, respectively, could be leading compounds for the synthesis of new anticancer drugs.

Supplemental Materials

Fig. S1 Molecular structure of compound **1** [31]

Fig. S2 Molecular structure of ligand **O1** (30% probability level)

Fig. S3 Unit cell of ligand **O1** with hydrogen bonding
(1: x, y, z; 2: ½ – x, ½ + y, ½ – z; 3: – x, – y, – z; 4: ½ + x, ½ – y, ½ + z)

Table S1 Selected torsion angle (º) in ligands **O1**, **O2**, and **O3**

Torsion angle (º)	O1	O2	O3
C6-S1-N1-C1 C2-S1-N1-C13 [a]	179.94(16)	179.6(3)	179.67(17)
N1-S1-C6-N3 N1-S1-C2-N3	179.64(16)	179.1(3)	-179.08(17)
S1-N1-C5-C4 S1-N1-C1-C10	-178.98(14)	-178.9(2)	-179.23(15)
C1-N1-C5-N2 C13-N1-C1-N2	-179.79(16)	179.7(3)	179.69(17)
C5-N2-C6-N3 C1-N2-C2-N3	-179.42(17)	179.4(3)	179.14(19)
C7-N3-C6-S1 C3-N3-C2-S1	-0.3(2)	-0.9(4)	-0.9(2)
C7-N3-C6-N2 C3-N3-C2-N2	179.26(17)	178.7(3)	179.92(18)
C6-N3-C7-O1 C2-N3-C3-O1	1.7(3)	0.0(5)	-1.1(3)
C6-N3-C7-C8 C2-N3-C3-C4	-177.36(16)	179.8(3)	178.82(18)
O1-C7-C8-C9 O1-C3-C4-C9	178.75(17)	-1.1(5)	-177.3(2)
N3-C7-C8-C9 N3-C3-C4-C5	-2.1(3)	179.2(3)	-176.38(19)

[a] First molecule in **O3**

Table S2 Complete information about bond length (Å) and angle (º) in complexes **C2** and **C3**

bond length (Å)	C2	C3	bond angle (º)	C2	C3
Cu1-N2	1.988(2)	1.990(2)	N2-Cu1-N2#1/2B	180.0	168.33(9)
Cu1-N2#1/2B	1.988(2)	1.996(2)	N2-Cu1-Cl1	91.10(6)	91.92(7)
Cu1-Cl1	2.2637(14)	2.2356(10)	N2#1/2B-Cu1-Cl1	88.90(6)	91.37(7)
Cu1-Cl1#1/Cl2	2.2637(14)	2.2544(10)	N2-Cu1-Cl1#1/Cl2	88.90(6)	89.74(7)
S1-C6	1.754(2)	1.747(3)	N2#1/2B-Cu1-Cl1#1	91.10(6)	88.55(7)
S1-N1	1.795(2)	1.809(2)	Cl1-Cu1-Cl1#1/Cl2	180.0	171.94(4)
S1-O1	2.124(2)	2.076(2)	C6-S1-N1	85.53(10)	85.60(13)
N1-C5	1.361(3)	1.353(3)	C6-S1-O1	79.71(9)	80.43(12)
N1-C1	1.364(3)	1.368(3)	N1-S1-O1	165.22(7)	165.97(10)
N2-C6	1.333(3)	1.331(3)	C7-O1-S1	105.68(15)	106.36(18)
N2-C5	1.362(3)	1.363(3)	C5-N1-C1	121.4(2)	122.6(3)
N3-C6	1.328(3)	1.331(3)	C5-N1-S1	112.92(14)	112.13(19)
N3-C7	1.345(3)	1.344(3)	C1-N1-S1	125.63(15)	125.2(2)
S1B-C6B		1.754(3)	C6-N2-C5	112.73(18)	112.4(2)
S1B-N1B		1.784(2)	C6-N2-Cu1	117.29(14)	120.98(19)
S1B-O1B		2.188(2)	C5-N2-Cu1	129.87(15)	126.64(19)
N1B-C5B		1.360(3)	C6-N3-C7	111.69(19)	110.8(2)
N1B-C1B		1.368(3)	C2-C1-N1	119.4(2)	117.5(3)
N2B-C6B		1.325(3)	C6B-S1B-N1B		86.16(12)
N2B-C5B		1.359(3)	C6B-S1B-O1B		78.82(11)
N3B-C6B		1.324(3)	N1B-S1B-O1B		164.97(9)
N3B-C7B		1.354(3)	C7B-O1B-S1B		104.71(17)
			C5B-N1B-C1B		122.5(2)
			C5B-N1B-S1B		112.17(18)
			C1B-N1B-S1B		125.30(19)
			C6B-N2B-C5B		112.7(2)
			C6B-N2B-Cu1		114.82(18)
			C5B-N2B-Cu1		131.95(18)
			C6B-N3B-C7B		112.4(2)
			C2B-C1B-N1B		117.6(3)

Acknowledgments

We are grateful to Islamic Azad University, Shahr-Ray branch, for their support. We also thank Dr. Ali Reza Fouromadi for his help.

References

[1] D. L. McMinn, Y. Rew, A. Sudom, S. Caille, M. Degraffenreid, X. He, R. Hungate, B. Jiang, J. Jaen, L. D. Julian, J. Kaizerman, P. Novak, D. Sun, H. Tu, S. Ursu, N. P. Walker, X. Yan, Q. Ye, Z. Wang and, J. P. Powers, *Bioorg. Med. Chem. Lett.*, 2009, **19**, 1446–1450.
[2] R. J. Knox, F. Friedlos, M. Jarman and J. J. Roberts, *Biochem. Pharmacol.*, 1988, **37**, 4661–4669.
[3] P. A. C. Bragay, D. A. P. Dos Santos, M. F. D. G. F. DA Silva, P. C. Vieira, J. B. Fernandes, P. J. Houghton and R. Fang, *Nat. Prod. Res.*, 2007, **21**, 47–55.
[4] C. Jason, D. Quinn, H. Garret and K. Fred, *Differential tumour cytotoxicity compounds and compositions*, US 7125997, 2006.
[5] E. Kjellen, J. Wennerberg and R. Pero, Br. *J. Cancer*, 1989, **59**, 247–250.
[6] S. Lybak, E. Kjellén, J. Wennerberg and R.W. Pero, *Int. J. Radicat. Oncol., Biol. Phys.*, 1990, **19**, 1419–1424.
[7] V. Chandregowda, A. Kush and G. C. Reddy, *Eur. J. Med. Chem.*, 2009, **44,** 2711–2719.
[8] M. Hemshekhar, M. S. Santhosh, K. Kemparaju and K. S. Girish, *Basic Clin. Pharmacol. Toxicol.*, 2012, **110**, 122–132.
[9] A. A. Hamed, A. K. El-Ziaty, A. A. Abdalha, S. A. Shiba Abdul-Hafeedh and A. Abdullha, *World Appl. Sci. J.*, 2012, **19**, 688–698.
[10] N. A. Mohamed, M. M. Anwar, W. S. El-serwy and M. Elsherbiny, *Der Pharma Chem.*, 2012, **4**, 2055–2067.
[11] S. Mokhtaria, M. Mosaddegh, M. Hamzeloo Moghadam, Z. Soleymani, S. Ghafari and F. Kobarfarda, *Iranian J. Pharma. Res.*, 2012, **11**, 411–421.
[12] Y. Xiea, X. Chenb, J. Qinc, X. Kongd, F. Yed, Y. Jianga, C. Luod, H. Liud, H. Jiangd and R. Marmorsteinc, *Bioorg. Med. Chem. Lett.*, 2013, **23**, 2306–2312.
[13] A. J. Kraker, C. A. Mizzen, B. G. Hartl, J. Miin, C. D. Allis and R. L. Merriman, *Mol. Cancer. Ther.*, 2003, 2, 401–408.
[14] I. Koutsounas, C. Giaginis and S. Theocharis, *World J. Gastroenterol.*, 2013, **19,** 1173–1181.
[15] S. Flis, A. Gnyszka, K. Flis and J. Spławiński, *Eur. J. Pharmacol.*, 2010, **627**, 26–32.
[16] G. Nagalakshmi, T. K. Maity and B. C. Maiti, *Pharmacologyonline*, 2013, **1**, 58–76.
[17] P. F. Neumann and M. Silverberg, *Nature*, 1967, **213**, 775–779.
[18] J. R. Sorenson, *J. Med. Chem.*, 1976, **19**, 135–148.
[19] D. Kovala-Demertzi, *J. Inorg. Biochem.*, 2000, **79**, 153–157.
[20] D. K. Johnson, T. B. Murphy and N. J. Rose, *Inorg. Chim. Acta*, 1982, **67**, 159–165.
[21] T. Tanaka, K. Yukawa and N. Umesaki, *Oncol. Rep.*, 2005, **14**, 1365–1369.
[22] D. Wang and S. J. Lippard, *Nat. Rev. Drug Discov.*, 2005, **4**, 307–320.
[23] A. M. Angeles-Boza, P. M. Bradley, P. K. L. Fu, S. E. Wicke, J. Bacsa, K. M. Dunbar and C. Turro, *Inorg. Chem.*, 2004, **43**, 8510–8519.
[24] H. Zhanga, C. S. Liub, X. H. Bub and M. Yanga, *J. Inorg. Biochem.*, 2005, **99,** 1119–1125.

[25] L. Jia, J. Shi, Z.H. Sun, F. F. Li, Y. Wang, W.N. Wua and Q. Wang, *Inorg. Chim. Acta*, 2012, 391, 121–129.
[26] C. Marzano, M. Pellei, F. Tisato and C. Santini, *Anti-Cancer Agents Med. Chem.*, 2009, **9**, 185–211.
[27] B. M. Zeglis, V. Divilov and J. S. Lewis, *J. Med. Chem.*, 2011, **54**, 2391–2398.
[28] D. S. Raja, N. S. P. Bhuvanesh and K. Natarajan, *J. Biol. Inorg. Chem.*, 2012, **17**, 223–227.
[29] G. M. Sheldrick, SADABS Version 2.03, University of Göttingen, Germany, 2001.
[30] G. M. Sheldrick, SHELXS-97 and SHELXL-97, University of Gottingen, Germany, 1997.
[31] W. Kaminsky, K. I. Goldberg and D. X. West, *J. Mol. Struct.*, 2002, **605**, 9–15.
[32] T. Mosmann, *J. Immunol. Methods*, 1983, **65**, 55–63.
[33] W. C. Emken, K. W. Hedberg and J. C. Decius, *Spectrochim. Acta, Part A*, 1997, **53**, 207–216.
[34] A. Tadjarodi, F. Adhami, Y. Hanifehpour, M. Yazdi, Z. Moghaddamfard and G. Kickelbick, *Polyhedron*, 2007, **26**, 4609–4618.
[35] D. X. West, J. K. Swearingen, A. K. Hermetet and L. J. Ackerman, *J. Mol. Struct.*, 2001, **562**, 95–105.
[36] J. Valdés-Martínes, S. Hernández-Ortega, G. Espinosa-Perez, C. A. Presto, A. K. Hermetet, K. D. Haslow, L. J. Ackerman, L. f. Szczepura, K. I. Goldberg, W. Kaminsky and D. X. West, *J. Mol. Struct.*, 2002, **608**, 77–87.
[37] D. X. West, L. F. Szczepura, J. M. Giesen, W. Kaminsky, J. Kelley and K. I. Goldberg, *J. Mol. Struct.*, 2003, **646**, 95–102.
[38] D. J. Che, G. Li, Z. Yu, D. P. Zou and C. X. Du, *Inorg. Chem. Commun.*, 2000, **3**, 537–540.
[39] S. Ahmad, A. A. Isab and W. Ashraf, *Inorg. Chem. Commun.*, 2002, **5**, 816–819.
[40] D. Whittaker, *Interpreting Organic Spectra*, RSC, London, 2000.
[41] B. Koren, B. Stanovnika and M. Tislera, *Org. Prep. Proceed. Int.*, 1975, **7**, 55**–**59.
[42] I. Leban, *Acta Cryst. B*, 1976, **32**, 1601–1604.
[43] C.W. Cheung and S.L. Buchwald, *J. Org. Chem.*, 2012, 77, 7526–7537.
[44] O. Das and T. Kantipaine, *J. Chem. Sci.*, 2012, **124**, 1269–1273.
[45] G. Li, D. J. Che, Z. F. Li, Y. Zhu and D. P. Zou, *New J. Chem.*, 2002, **26**, 1629–1633.
[46] R.G. Pearson, *J. Am. Chem. Soc.*, 1963, **85**, 3533**–**3539.
[47] M. Ghassemzadeh, F. Adhami, M. M. Heravi, A. Taeb, S. Chitsaz and B. Neumüller, *Z. Anorg. Allg.*, 2002, 628, 2887–2893.
[48] V. C. Copeland, W. Hatfield and D. Hodgson, *Inorg. Chem.,* 1973, **12**, 1340–1343.
[49] U. P. Chaudhuri, D. R. Powell and R. P. Houser, *Inorg. Chim. Acta*, 2009, **362**, 2371–2378.
[50] D. O. Ivashkevich, A. S. Lyakhov, S.V. Voitekhovich and P. N. Gaponik, *Acta Cryst.*, 2002, **C58**, m563**–**m564.
[51] P. Talukder, A. Datta, S. Mitra and G. Rosair, *Z. Naturforsch.*, 2004, **59b**, 655**–**660.
[52] J. G. Tojal, A. G. Orad, J. L.Serra, J. L. Pizarro, L. Lezama, M. I. Arriortua and T. Rojo, *J. Inorg. Biochem.*, 1999, **75**, 45**–**54.

[53] L. Gutierrez, G. Alzuet, J. Borrás, M. L. González, F. Sanz and A. Castineiras, *Polyhedron*, 2001, 20, 703–709.
[54] V. V. Bon, *Acta Cryst.*, 2010, C**66**, m300–m302.
[55] R. A. Ahmadi, F. Hasanvand, G. Bruno, H. A. Rudbari and S. Amani, *ISRN Inorg. Chem.*, 2013, **2013**, 1–7.
[56] K. R. Hande, *J. Cancer*, 1998, **34**, 1514–1521.
[57] S. C. Sweetman, *Martindale: The Complete Drug Reference*, Pharmaceutical Press, 37th Ed. 2011.

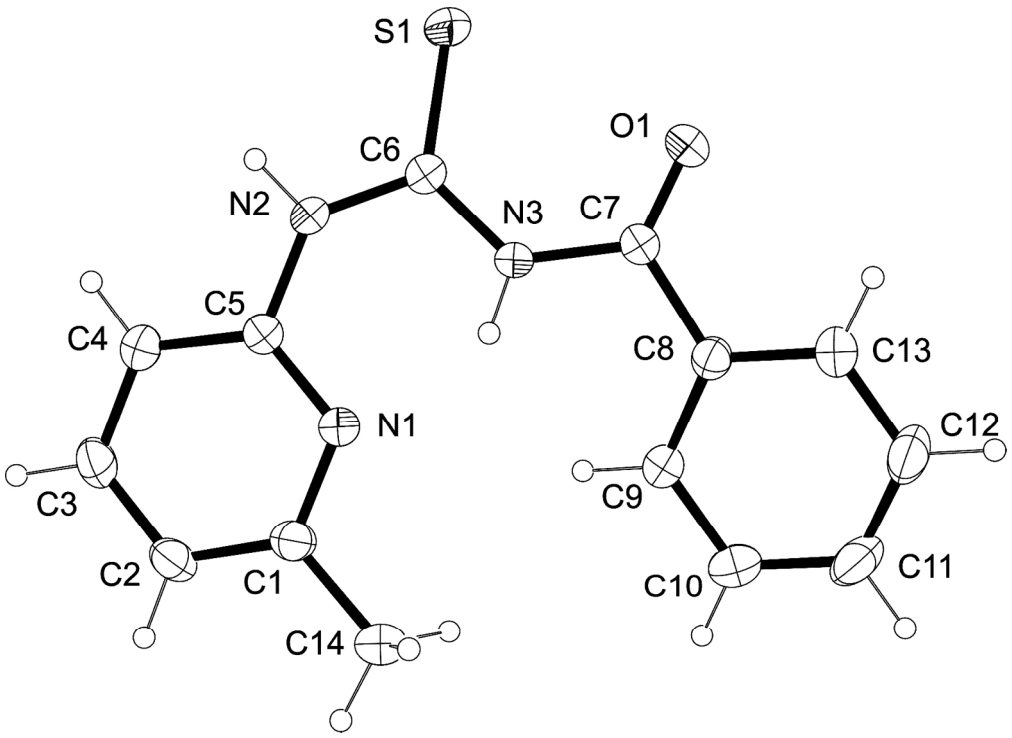

499x362mm (96 x 96 DPI)

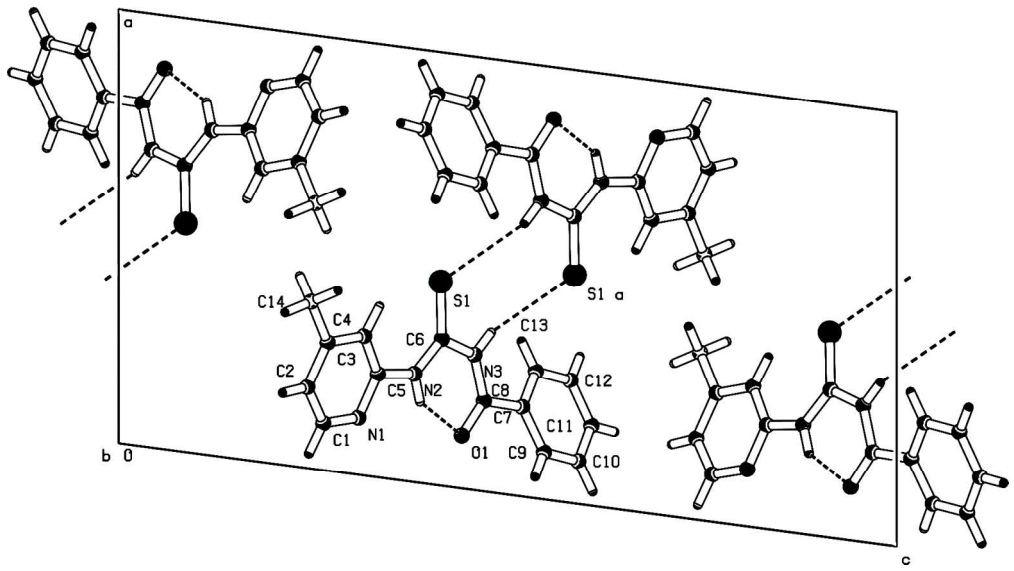

499x277mm (96 x 96 DPI)

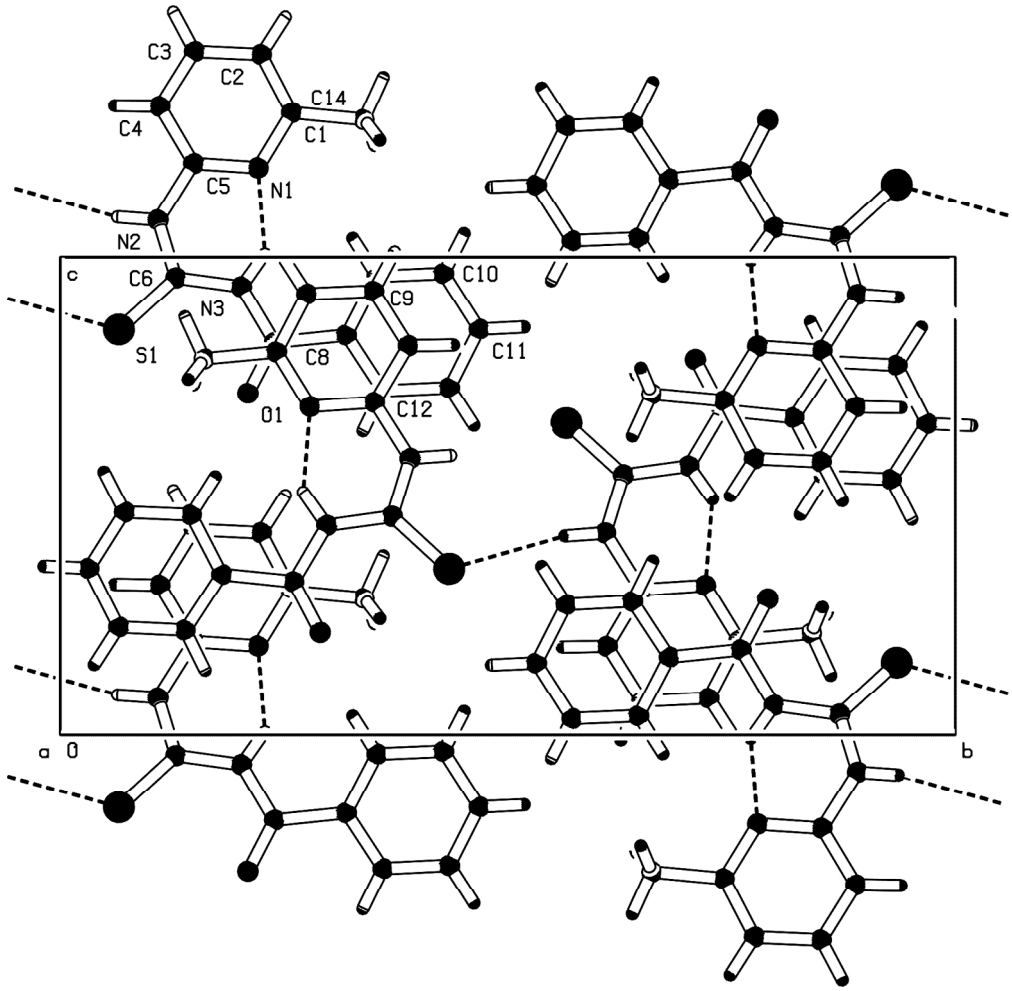

499x489mm (96 x 96 DPI)

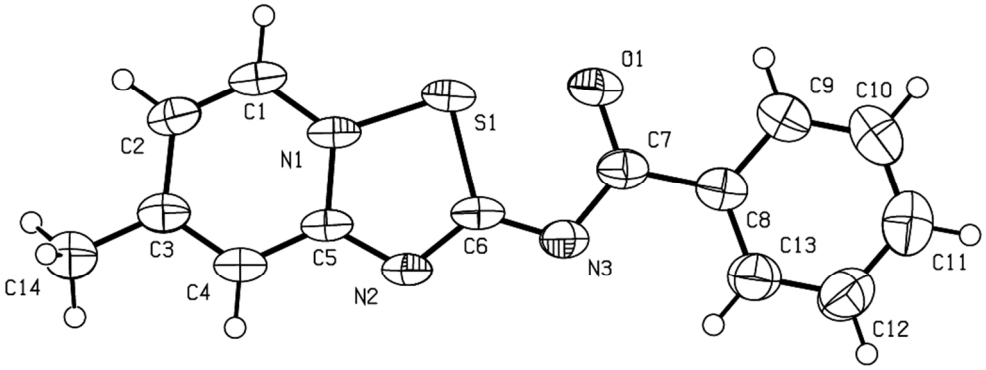

281x103mm (96 x 96 DPI)

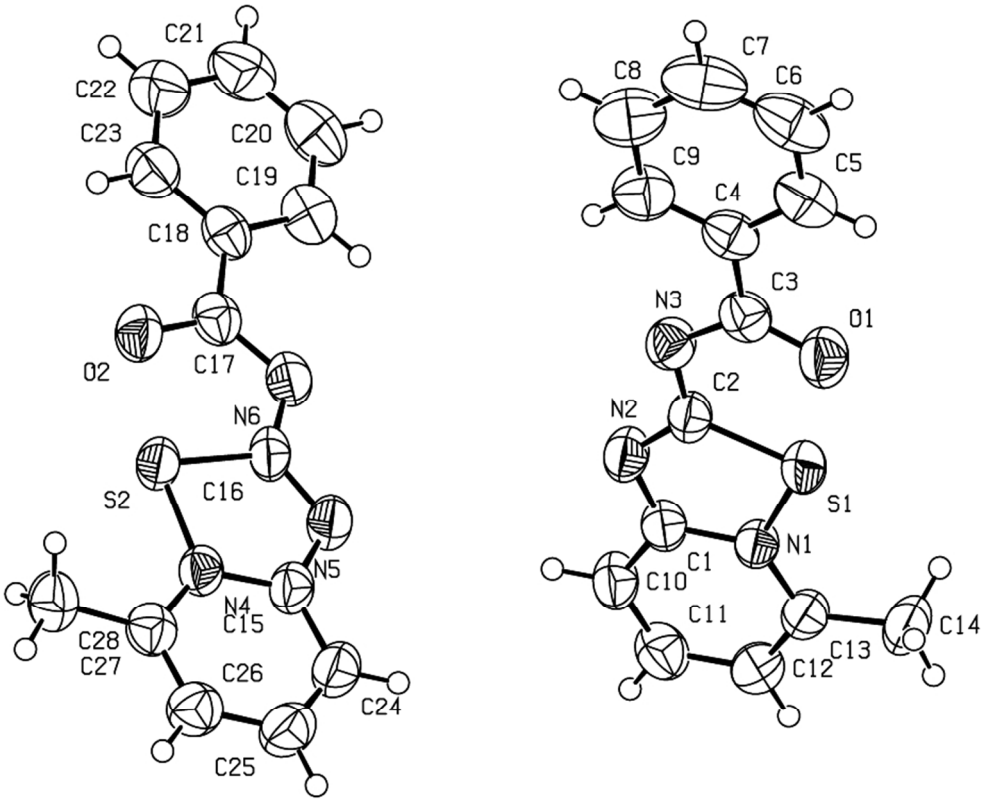

248x204mm (96 x 96 DPI)

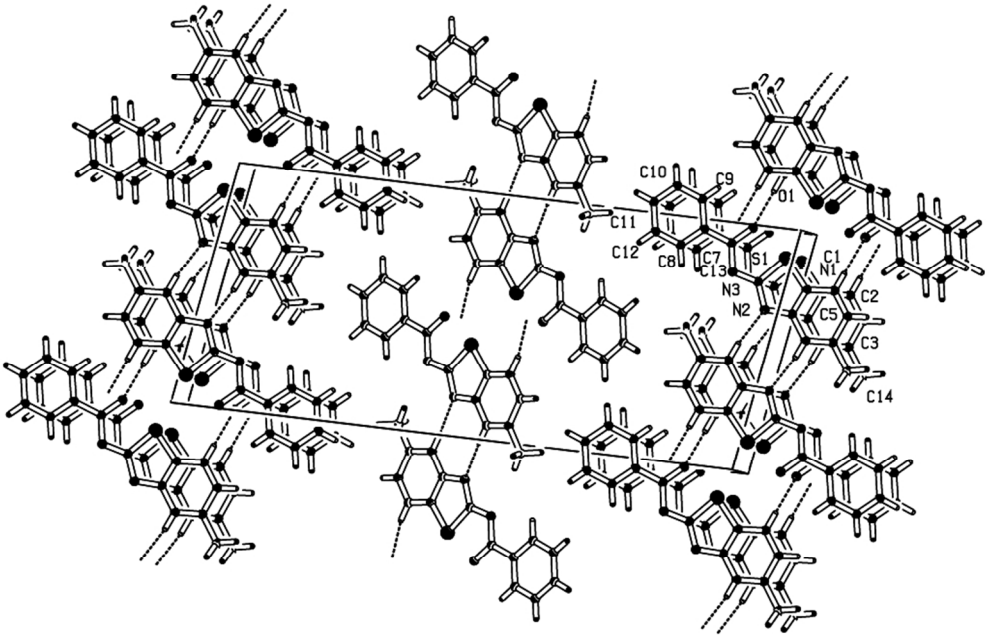

274x185mm (96 x 96 DPI)

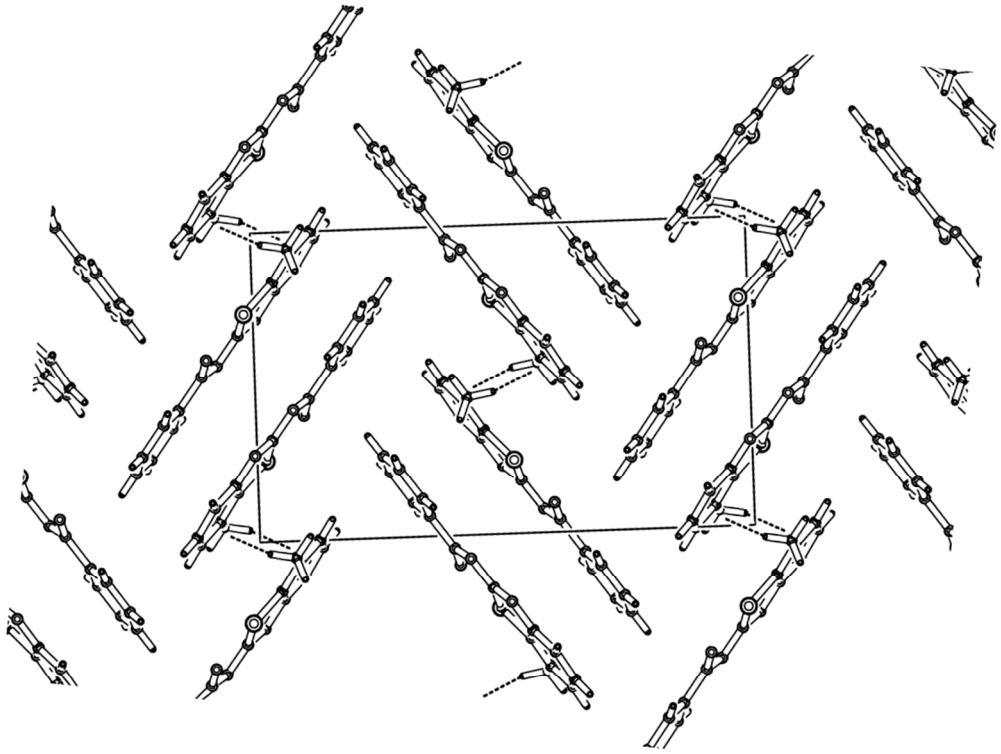

313x250mm (96 x 96 DPI)

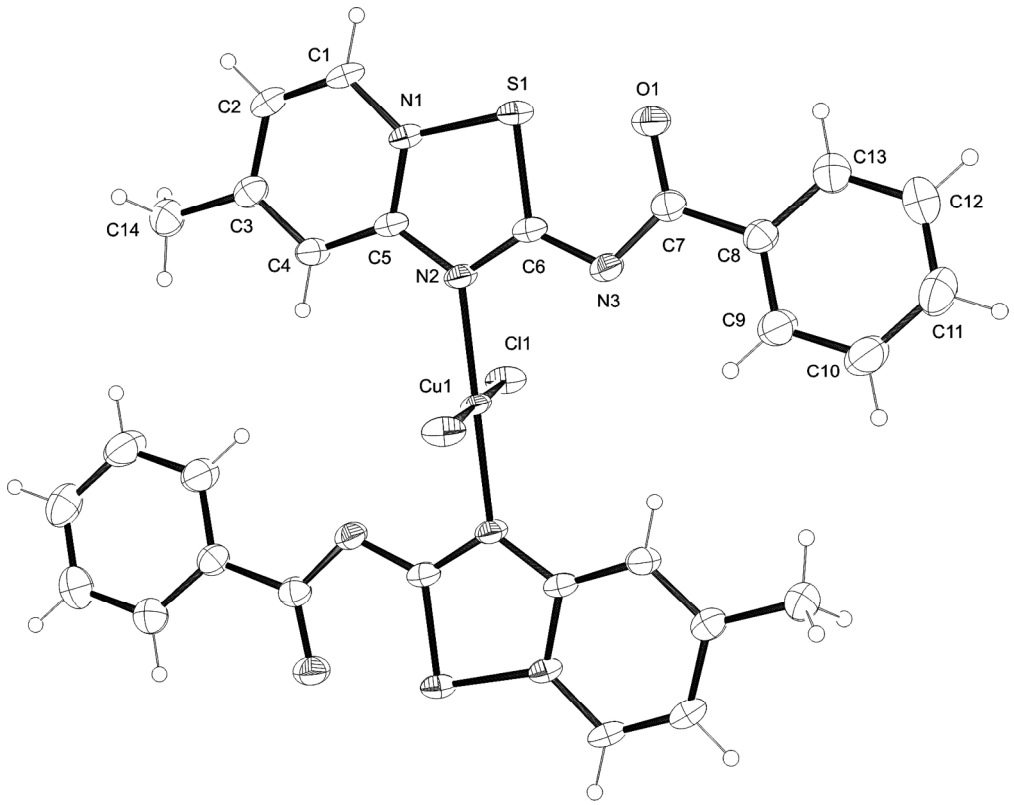

499x396mm (96 x 96 DPI)

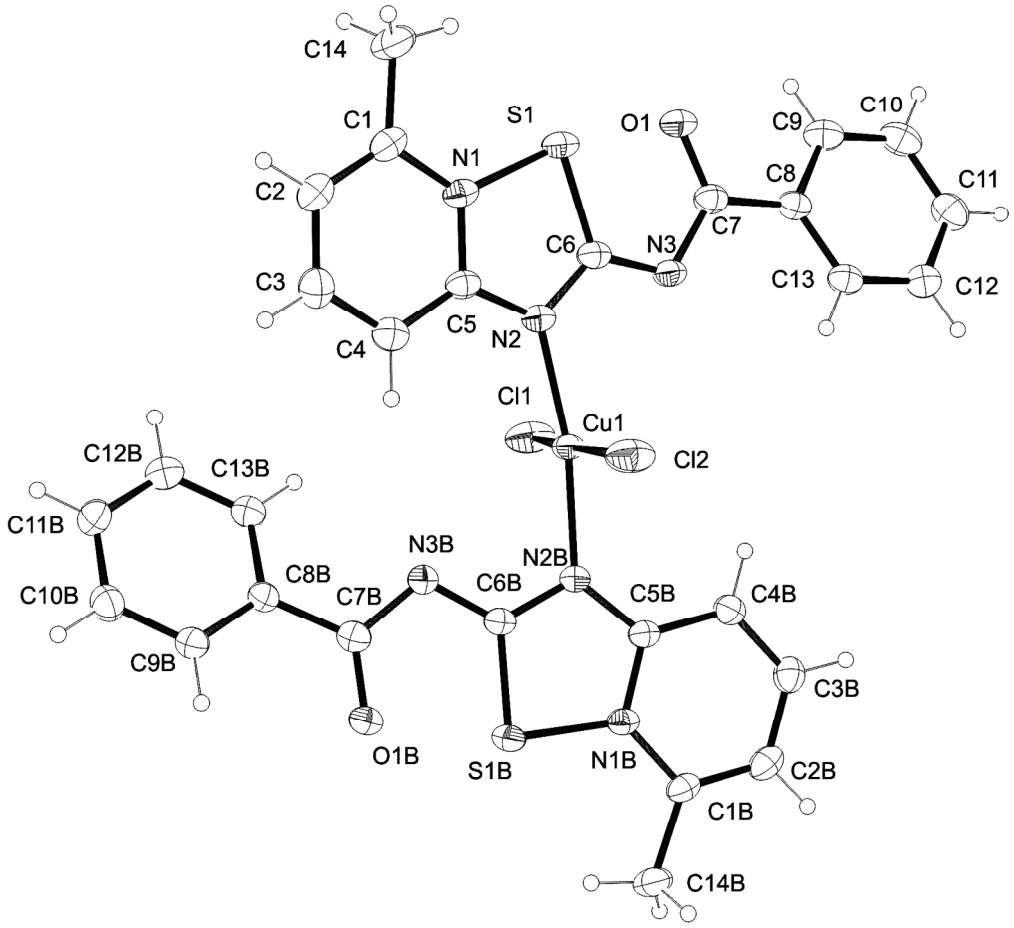

499x457mm (96 x 96 DPI)

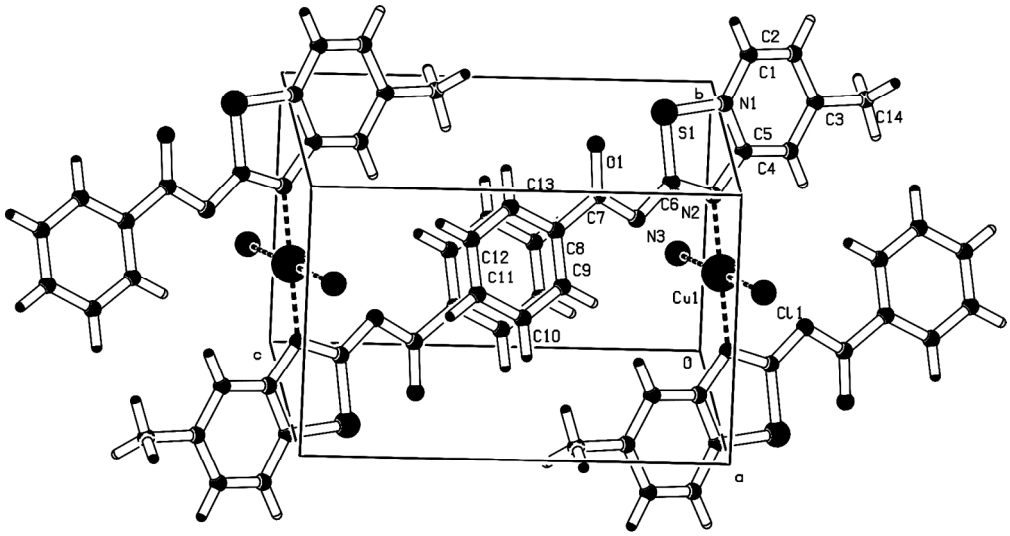

499x272mm (96 x 96 DPI)

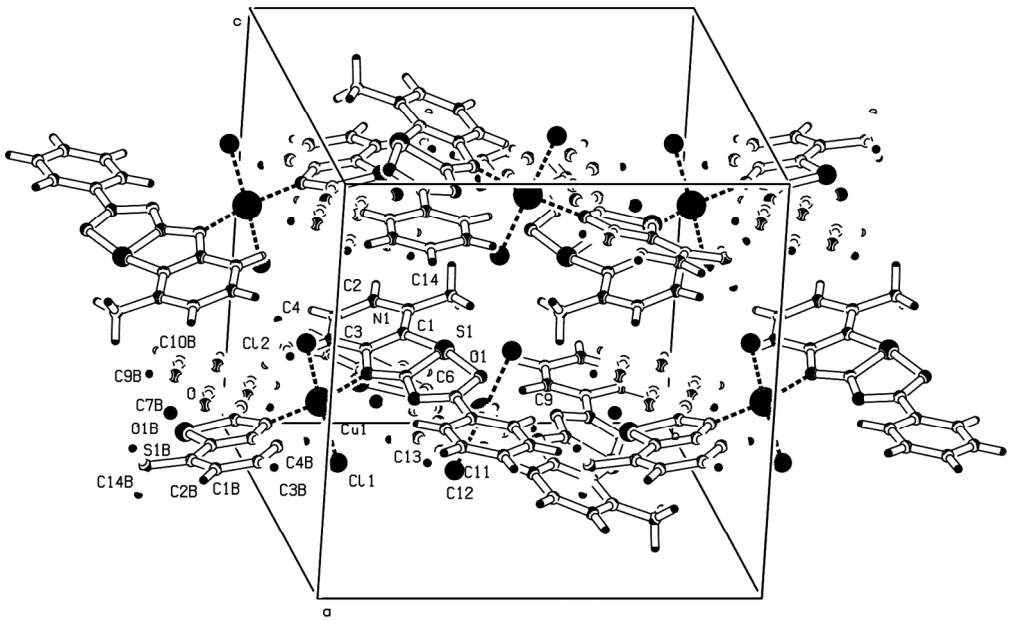

499x314mm (96 x 96 DPI)

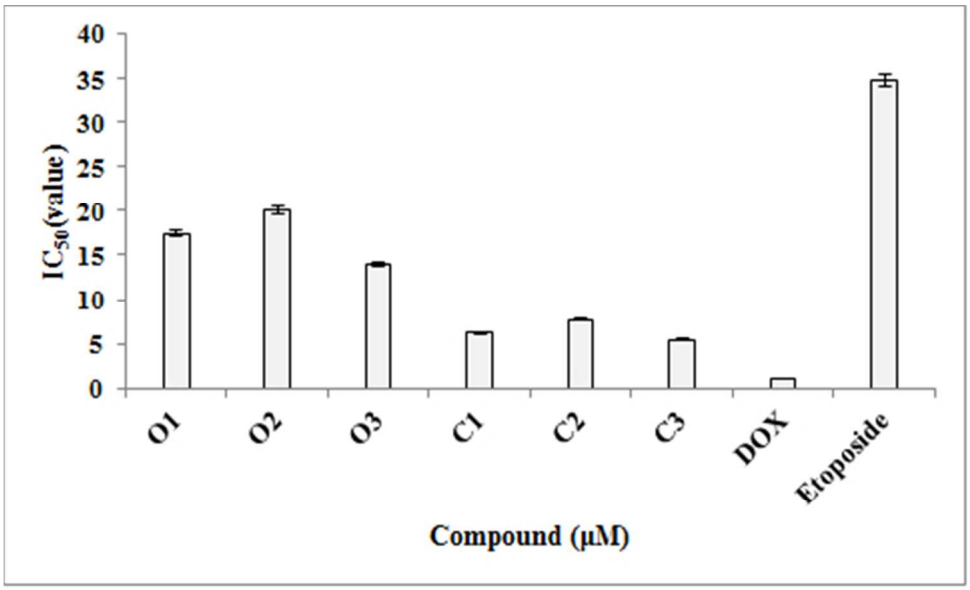

128x78mm (96 x 96 DPI)

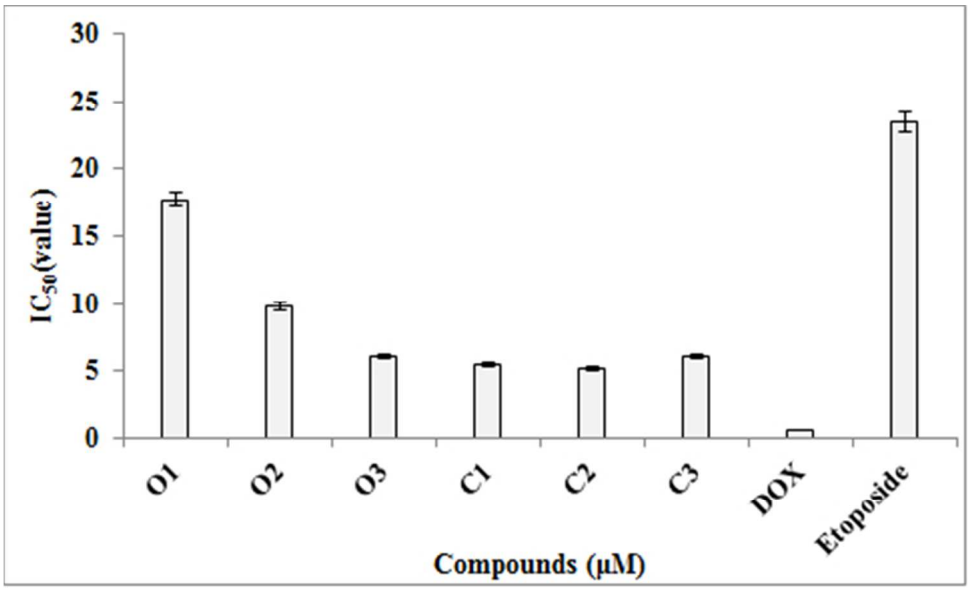

128x78mm (96 x 96 DPI)

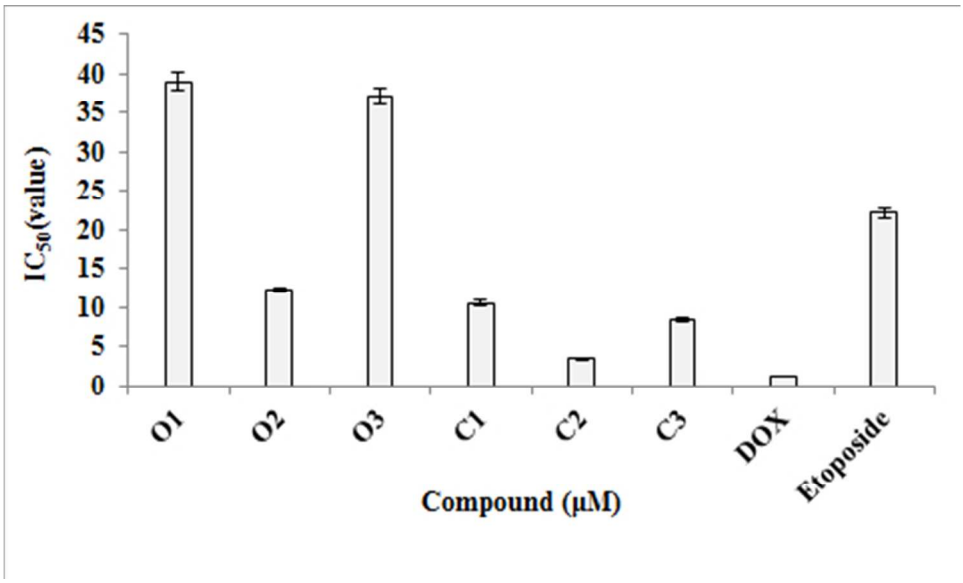

126x75mm (96 x 96 DPI)

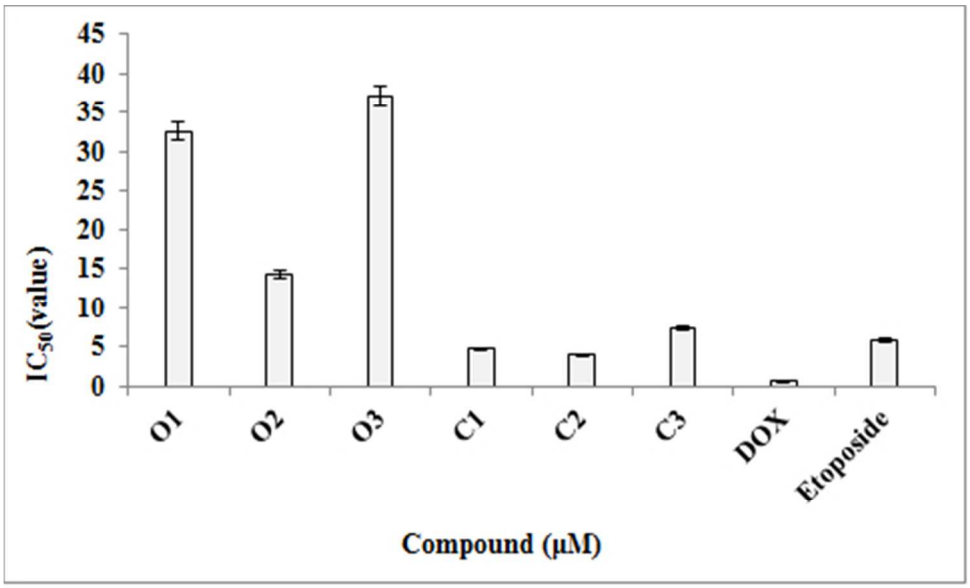

128x78mm (96 x 96 DPI)

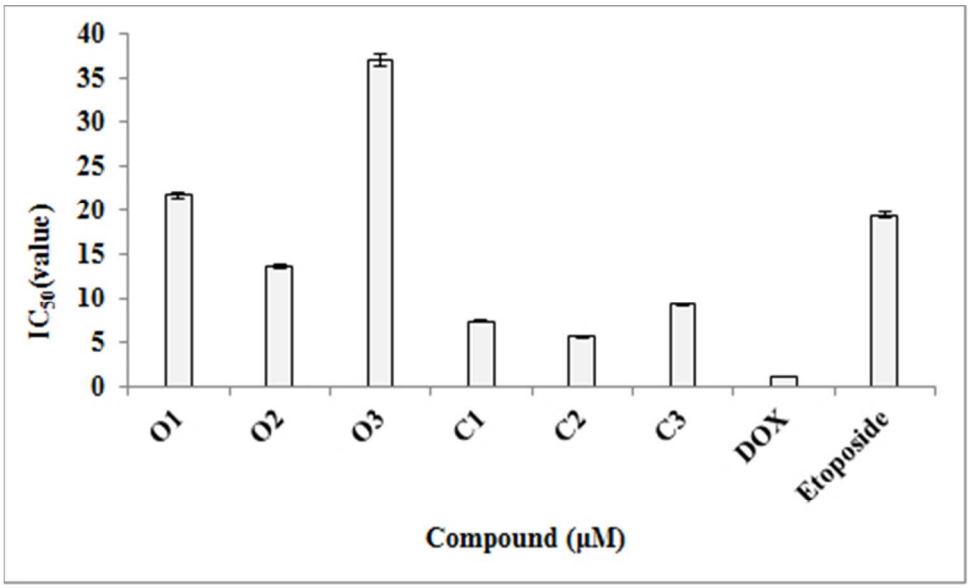

128x78mm (96 x 96 DPI)

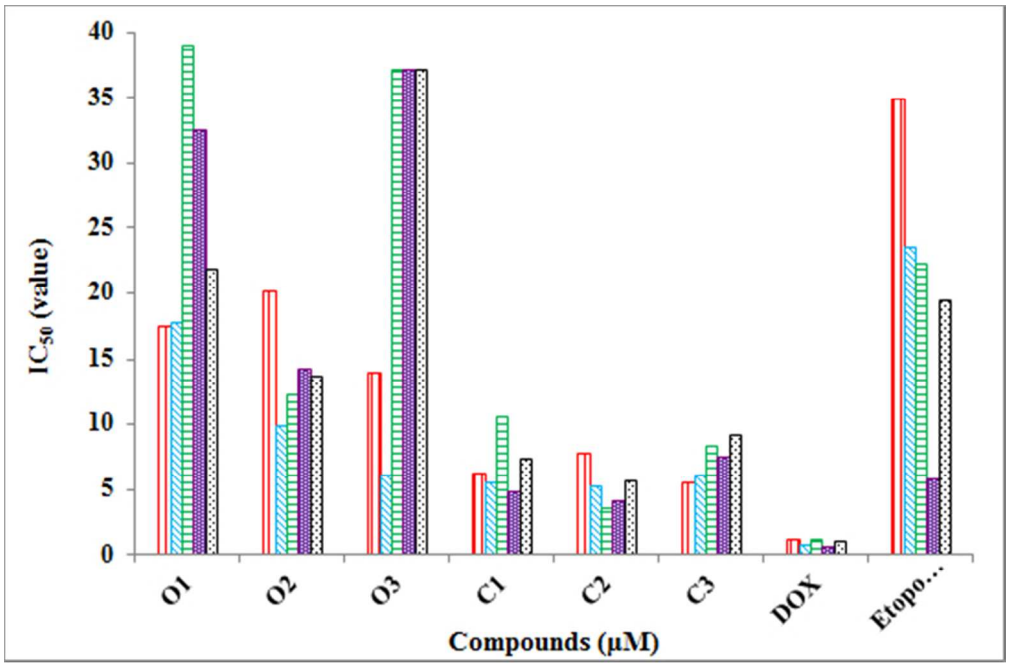

144x94mm (96 x 96 DPI)